The Tectonic and Metallogenic Framework of Myanmar: A Tethyan Mineral System

Nicholas J. Gardiner[1,9*], Laurence J. Robb[1], Christopher K. Morley[2,3], Michael P. Searle[1], Peter A. Cawood[4], Martin J. Whitehouse[5], Christopher L. Kirkland[6], Nick M.W. Roberts[7], Tin Aung Myint[8]

1. Department of Earth Sciences, University of Oxford, Oxford OX1 3AN, United Kingdom.

2. Department of Geological Sciences, Chiang Mai University, Thailand.

3. PPT Exploration and Production, Vibhavadi-Rangsit Road, soi 11, Bangkok, Thailand 10900.

4. Department of Earth Sciences, University of St Andrews, North Street, St Andrews KY16 9AL, United Kingdom

5. Swedish Museum of Natural History, and Nordic Center for Earth Evolution, Box 50007, SE-104 05 Stockholm, Sweden.

6. Centre for Exploration Targeting – Curtin Node, Department of Applied Geology, Western Australian School of Mines, Curtin University, Perth, WA 6845, Australia.

7. NERC Isotope Geosciences Laboratory, British Geological Survey, Keyworth, Nottingham NG12 5GG, United Kingdom.

8. Department of Geology, Mandalay University, Mandalay, Myanmar.

9. Presently at: Centre for Exploration Targeting – Curtin Node, Department of Applied Geology, Western Australian School of Mines, Curtin University, Perth, WA 6845, Australia.

*Corresponding author. E-mail address: nicholas.gardiner@curtin.edu.au

Abstract

Myanmar is perhaps one of the World's most prospective but least explored minerals jurisdictions, containing important known deposits of tin, tungsten, copper, gold, zinc, lead, nickel, silver, jade and gemstones, in addition to a substantial hydrocarbon endowment. A scarcity of recent geological mapping available in published form, coupled with an unfavourable political climate has resulted in the underdeveloped exploitation of its mineral resources. As well as representing a potential new search space for a range of commodities, many of Myanmar's known existing mineral deposits remain highly prospective. Myanmar lies at a crucial geologic juncture, immediately south of the Eastern Himalayan Syntaxis, however remains geologically enigmatic. Its Mesozoic-Recent geological history is dominated by several orogenic events representing the closing of the Tethys Ocean. We present new zircon U-Pb age data related to several styles of mineralization within Myanmar. We outline a tectonic model for Myanmar from the Late Cretaceous onwards, and document nine major mineralization styles representing a range of commodities found within the country. We propose a metallogenetic model that places the genesis of many of these metallotects within the framework of the subduction and suturing of Neo-Tethys and the subsequent Himalayan Orogeny. Analysis of this model suggests that the principal orogen-scale geological factor that governs the type and distribution of mineral deposit types in Myanmar is its evolving geodynamic setting. Temporal overlap of favourable conditions for the formation of particular deposit types permits the genesis of differing metallotects during the same orogenic event. We suggest the evolution of these favourable conditions and resulting genesis of much of

Myanmar's mineral deposits, represents a single, evolving, mineral system: the subduction and suturing of the Neo-Tethys.

1. Introduction

Myanmar (Burma) is a highly prospective but poorly explored orogenic terrane. Despite limited past exploration, it is known to be well endowed in a diversity of mineral deposits, hosting important known reserves of varying economic significance of tin, tungsten, copper, gold, zinc, lead, nickel, silver, jade and gemstones (e.g., Barber et al., 2016; Chhibber, 1934; Coggin Brown, 1936; Gardiner et al., 2014; Griffith, 1956; Soe Win and Malar Myo Myint, 1998). The country contains ore deposits of global significance, notably Monywa (copper) and Bawdwin (lead-zinc); it produces some of the World's finest rubies sourced from Mogok; and is the principal global source of true jade (jadeite). A majority of Myanmar's known mineral endowment was discovered and developed during the early part of the 20th Century, however there has been comparatively little recent exploration and discovery. There is a lack of available published geological literature on Myanmar, and the country is underdeveloped with regards to the exploitation of its natural resources (e.g., Cox et al., 1981). However, as well as being a potential new search space for a range of commodities, many of its known mineral deposits remain highly prospective due to a past political and economic climate that has rendered much of its extractive industry as essentially artisanal.

Myanmar lies at a crucial geologic juncture where the main Tethys-related suture zones swing south around the Eastern Himalayan Syntaxis into Southeast Asia, with the consequence that the region has experienced an increasingly oblique collisional geometry over its Mesozoic-

Cenozoic orogenic history. An understanding of both the genesis of Myanmar's mineralization, and of its mineral potential, can only be fully realized with an understanding of its tectonic history. Myanmar, however, remains geologically enigmatic, in part due to its relative political and scientific isolation over the past half century. A number of foreign-led projects have contributed over the years to the understanding of the geological history of Myanmar: key regional re-mapping by the United Nations Directorate of Geological Survey and Mineral Exploration team (UNDP, 1978); missions by several governmental agencies (principally the Bundesanstalt für Geowissenschaften und Rohstoffe (BGR); the Institute of Geological Sciences (IGS, now BGS); and in the 1980s the Australian Development Assistance Bureau); and ongoing works by notable individuals. However, little modern dating work, using current palaeontological or radiometric techniques, or significant and accessible geological (re)mapping, has emerged from the country. Therefore, there remains considerable uncertainty around the configuration, nature and timing of major Tethyan-related tectonic events, which renders discussions on Myanmar's metallogenesis somewhat equivocal.

We propose that Myanmar has experienced a Late Mesozoic-Cenozoic orogenic event that operated over a reasonably short period of time with little overprinting complexity, yet an orogenic system that was potentially responsible for the genesis of a significant range of mineral deposits. The preservation potential of Myanmar's near-surface, epizonal mineral deposits is relatively high due to its recent geological evolution. Myanmar therefore may represent an exceptional scientific test piece, affording workers the

100 opportunity to use the tectonothermal evolution of the country to explore
101 fundamental questions on the relationship between a complex and evolving
102 orogen and the resulting metallogenesis.

103 In this paper we review the range of known mineral deposits
104 found within Myanmar, and place them within a space-time construct that
105 reflects Myanmar's Mesozoic-Cenozoic geological history. We argue for a
106 simple tectonic scenario: the subduction and suturing of the Neo-Tethys and
107 the ensuing Himalayan Orogeny, and present a metallogenic model for
108 Myanmar that accommodates the potential genesis of up to nine major
109 metallotects within this orogenic framework. Finally, we use this model to
110 make large-scale observations regarding the progression of orogeny and
111 concomitant mineral deposit genesis. This thesis, if correct, would place the
112 genesis of a majority of Myanmar's mineral deposits within a single, evolving,
113 mineral system: the subduction and suturing of the Neo-Tethys.

114 *1.1. A Short History of Mining and Exploration in Myanmar*

115 Although artisanal mining and smelting of tin, silver and other
116 deposits, by both Burmese and Chinese, occurred within what is now modern-
117 day Myanmar during mediaeval times, much of Myanmar's known minerals
118 resources were developed and exploited during the second half of the 19th
119 century into the 20th century. Under British colonial control, the early 20th
120 century showed a major upturn and industrialization of the Burmese mining
121 industry, with many major mines of a variety of commodities being developed
122 during this time, largely producing for export. Myanmar was an important
123 producer of tungsten, a strategic war material, during the interwar period
124 (principally supplied by the Mawchi Mine), and of lead, zinc and silver from the

Bawdwin Mine in the Shan States. It was also a major supplier of tin. Much of colonial Burma was under military occupation by the Japanese during the Second World War, who operated some of the major mines during the period 1942-44. The post-war period saw the newly independent Burma continue to produce and export a range of commodities, although production never reached pre-war levels. In 1962, General Ne Win led a military coup entrenching the rule of the Burmese army, leading to the launch of the "Burmese Way to Socialism". This process pursued the full nationalization of the Burmese economy, and a policy of economic isolation from the rest of the World. The economic effects on the mining industry were profound: all mines in Burma were brought under government control, and many commodities only became available on the black market. This period hastened the decline of the Burmese mining industry and marked a shift into largely artisanal operations, still seen today.

In 1988 Myanmar passed foreign investment legislation allowing external financial and technological investment into country. Since then, and in contrast to the minerals industry, the oil and gas sector has seen significant overseas investment. In 1994 a new Mining Law was put into place, repealing colonial-era and post-independence legislation. The new law allowed prospecting, exploration and production permits. A revision of this mining law was signed in January 2016.

1.2. Mineral Systems

Mineral deposits are heterogeneously dispersed over both space and time, reflecting both the influence of geodynamic setting on mineralization, and the transient nature of the specific geological processes

that form ores (Begg et al., 2010; Cawood and Hawkesworth, 2013; Goldfarb et al., 2005). For many mineral systems the style and timing of tectonic events are fundamental for developing a suitable crustal architecture that accommodates mineralization. Therefore, by integrating the geodynamic evolution of a region with mineral systems theory (Fraser et al., 2007), we can place deposit models and deposit types within the context of earth evolution and provide a broad scale predictive framework for a terrane. A practical approach is to unpick an orogen on a time-integrated basis and chart the evolution of deposit types, and by inference, key mineral system elements, through the lifetime of the orogen. Due to the intricate relationships between mineral deposits and setting, such studies can ultimately better constrain the model of the orogenic system. In this paper we take this approach with Myanmar.

2. Geological Framework of Myanmar

2.1. Regional Tectonic Framework

The Mesozoic-Recent geology of Southeast Asia is dominated by the accretion of several continental micro-plates and island arc terranes that rifted from Gondwana, migrated and eventually sutured onto the South China Craton (reviews in Hall, 2012, and Metcalfe, 2013). This history of rifting and suturing represents the staged closing of the Tethys Ocean, rendering much of Southeast Asia a collage of continental blocks separated by suture zones (Fig. 1). Sibumasu (Metcalfe, 1984) is the continental microplate interpreted to underlie much of eastern and central Myanmar. Sibumasu possibly originated from the proto-Tethys margin of Gondwana, a

174 margin postulated as having been sited above an Andean-type subduction
175 setting during the early Palaeozoic (e.g., Cawood et al., 2007; Metcalfe,
176 2011b; Zhu et al., 2012). Cambro-Ordovician magmatism associated with this
177 subduction setting (e.g., Wang et al., 2013) has been proposed as being
178 responsible for the development of the Bawdwin Mine, a major Pb-Zn VMS-
179 type deposit now located within Sibumasu (review in Gardiner et al., 2016).
180 Sibumasu is interpreted to have rifted off from Gondwana in the Late
181 Carboniferous-Early Permian (Metcalfe, 2006), subsequently colliding with the
182 Indochina Terrane during the Indosinian Orogeny. Fig. 2 (taken from Metcalfe,
183 2011) is a palaeogeographic reconstruction of eastern Tethys during Jurassic-
184 Eocene times, highlighting the Sibumasu block accreted onto Indochina and
185 South China, and charting the development of the Neo-Tethys Ocean, and the
186 onset of the India-Asia collision.

187 Myanmar has been affected by at least two major Tethyan plate
188 collisions related to the closure of the Palaeo-Tethys and the Neo-Tethys
189 oceans, represented by the Triassic-Early Jurassic Indosinian and Cenozoic
190 Himalayan orogenies respectively. The result is that several major Tethyan-
191 related metamorphic belts extend from the Eastern Syntaxis southwards
192 across Myanmar, and which may be correlated with those lying further west
193 along the main India-Asia collision zone (Searle et al., 2016).

194 The Late Triassic closure of the Palaeo-Tethys and the collision
195 of Sibumasu with the mainland (Asia) Indochina terrane resulted in the
196 Indosinian Orogeny. The Palaeo-Tethyan suture zone is interpreted to lie in a
197 north-south band cutting through Yunnan, eastern Myanmar, central-western
198 Thailand and the central Malay Peninsula (Barr and Macdonald, 1991;

199 Gardiner et al., 2015a; Metcalfe, 2002, 2000; Mitchell, 1977; Ng et al., 2015;
200 Sone and Metcalfe, 2008; Zi et al., 2012). This suture zone forms the
201 boundary between two major north-south Mesozoic-age granite provinces that
202 run across much of Southeast Asia: the *Eastern Granite Belt* and the *Central*
203 *Granite Belt* of Cobbing et al. (1986). Mineralization processes associated
204 with Central Granite Belt magmatism are responsible for most of the extensive
205 tin deposits exploited in Malaysia and Thailand as both primary and placer
206 deposits (Cobbing et al., 1992; Hutchison and Taylor, 1978).

207 The early Eocene closure of the Neo-Tethys resulted in the
208 collision of the Indian Plate with Asia along the main convergent margin, and
209 the subsequent onset of the Himalayan Orogeny. Suturing between India and
210 Asia has been dated along the Indus Tsangpo (India-Asia) suture along the
211 main Himalayan-Karakoram collision zone at 50 Ma (Garzanti et al., 1987;
212 Green et al., 2008; Searle and Morley, 2011; Searle et al., 1988). Further
213 east, this suture zone wraps around the Eastern Himalayan Syntaxis at
214 Namcha Bawra, and is thought to reappear along the Mount Victoria-Kawlun
215 Belt in western Myanmar (see review in Searle et al., 2016). The Himalayan
216 Orogeny resulted in significant regional crustal thickening, and the formation
217 of major mountain belts, manifest in Myanmar as concomitant magmatism
218 and regional metamorphism (Mitchell, 1993; Morley, 2012; Searle and Morley,
219 2011; Sone and Metcalfe, 2008).

220 The collisional geometry along the main northern Himalayan
221 suture zone, driven by the continued northwards progression of the Indian
222 plate, is orthogonally convergent. For Southeast Asia, however, the ongoing
223 collision occurred within the framework of a clockwise rotation of accreted

Asiatic terranes around the Eastern Himalayan Syntaxis, which led to an increasingly oblique collision zone with time (e.g., Replumaz and Tapponnier, 2003). However, the amount of Cenozoic rotation varies considerably between different plate reconstructions, with the reconstructions of Hall (2012) and Zahirovic et al. (2014) suggesting much less clockwise rotation than the reconstruction of Replumaz and Tapponnier (2003). As a consequence, oblique collision for Myanmar specifically and Southeast Asia in general is an early feature of the deformation in the models of both Hall (2012), and Zahirovic et al. (2014). The oblique nature of the collision is reflected in a number of significant regional strike-slip faults that developed during the Palaeogene and Neogene, and which provided an accommodation of strain associated with this rotational history. The active tectonics of Myanmar is dominated by major strike-slip faulting along the right-lateral Sagaing Fault, and other strike-slip faults to the west (Maurin and Rangin, 2009), and strike-slip, thrust and normal fault earthquakes, associated with a relic subducted slab, dipping eastwards under Central Myanmar. Movement on the Sagaing Fault (Fig. 1), has been measured at a present-day ca. 1.8–2 cm/yr of strike-slip component (Maurin et al., 2010; Socquet et al., 2006; Vigny, 2003), a figure that accommodates approximately 50% of the current northwards progression of the Indian Plate. The Sagaing Fault extends south into the Andaman Sea, where it links to the Pliocene-Recent back-arc spreading centre.

2.2. Geological Provinces of Myanmar

Here we divide Myanmar into four major geological provinces from west to east (Fig. 3): the *Indo-Burman Ranges*, the *Wuntho-Popa Arc*, the *Mogok-Mandalay-Mergui Belt*, and the *Shan Plateau*.

The Indo-Burman Ranges in the far west comprise ophiolitic and Upper Triassic flysch outcropping both within the Mount Victoria Belt and elsewhere (e.g., Brunnschweiler, 1966). West of the Indo-Burman Ranges lies the effective margin of Asian continent (Ghose et al., 2014; Mitchell, 1993; Mitchell et al., 2012), which is shown through geophysical data to be a dextral strike-slip margin (Nielsen et al., 2004). The nature of the continental crust underlying western Myanmar is, however, disputed (see Section 5.2.2).

A 500 km-long arcuate N-S belt of Mesozoic to Neogene intrusive and volcanic rocks and Pliocene-Quaternary calc-alkaline stratovolcanoes (Mounts Popa, Taung Thonlon and Loimye) defines the Wuntho-Popa Arc (henceforth “WPA”). The WPA is a continental magmatic arc (Fig. 3) (Mitchell and McKerrow, 1975; UNDP, 1978). This comprises major Cretaceous-Eocene granodiorite intrusions and associated volcanic rocks, and middle Miocene rhyolites and dacites, principally outcropping in Mount Popa and inliers to the south (Barley et al., 2003; Khin Zaw, 1990; Mitchell and McKerrow, 1975; Mitchell et al., 2012). In places these assemblages are overlain by Quaternary basaltic andesites and pyroclastic flows (Maury et al., 2004; Stephenson and Marshall, 1984). The WPA exposes two principal inliers, surrounded by Oligocene-Recent shallow marine sedimentary rocks covering much of the Arc: the 160 km-long Wuntho-Banmauk segment in the north (UNDP, 1978), and the Monywa-Salingyi

segment in central Myanmar. These magmatic units intrude pre mid-Cretaceous pillow basalts, greenstones, and amphibolite and gneissic basement of undetermined age (Mitchell et al., 2011, 2012).

The WPA lies above the active easterly-dipping Burma Seismic Zone, where earthquakes have been recorded to depths of 230 km (Stork et al., 2008; review in Searle and Morley, 2011). Although it is uncertain whether the Burma Seismic Zone is underlain by a subducting slab of oceanic lithosphere, seismic receiver functions reveal that the Moho lies at 35-38 km depth beneath the southern Shillong Plateau (Mitra et al., 2005). Thus it seems probable that the Indo-Burman Ranges are underlain by continental crust that thins towards the east, with transitional oceanic lithosphere attached to the subducted plate along the Burma Seismic Zone.

The Mogok Metamorphic Belt (Searle and Ba Than Haq, 1964) is a north-south aligned belt of metamorphic rocks and granites that extends from the Andaman Sea through Mandalay northwards in an arcuate trend towards the Eastern Himalayan syntaxis (Fig. 3). It comprises a sequence of high-grade meta-sedimentary and meta-intrusive rocks, representing a regionally metamorphosed amphibolite-grade belt (Iyer, 1953; Mitchell et al., 2007; Searle et al., 2016, 2007). Zircon and monazite U-Pb dating has indicated that peak metamorphism is of Eocene age and younger (Searle et al., 2007). The adjacent Slate Belt (Mitchell et al., 2004) outcrops from Mandalay south towards Phuket, and is a predominantly late Palaeozoic succession of low-grade metasedimentary units; pebbly mudstones and wackes with occasional limestones, collectively defined as the Mergui Group (Mitchell, 1992). The Mogok Metamorphic Belt and Slate Belt together lie to

296 the west of the Paung Laung-Mawchi Zone (Fig. 1). The Paung Laung-
297 Mawchi Zone is interpreted by Mitchell et al. (2012) as a possible pre-Permian
298 suture, consisting of folded late Jurassic to mid-Cretaceous marine clastic
299 sedimentary rocks and limestones. Intruding into both of these units is
300 Myanmar's second major magmatic belt, a north-south trending belt of
301 granitoids emplaced from the Late Cretaceous to at least Eocene times
302 (Barley et al., 2003; Cobbing et al., 1992; Mitchell et al., 2012; Searle et al.,
303 2007). This has been variously termed the Western Province (Cobbing et al.,
304 1992) - which is a confusing term within the context of Myanmar as it lies to
305 the central-east of the country - or the Central Granitoid Belt (e.g., Khin Zaw,
306 1990). Here we refer to the entire zone comprising Mogok Metamorphic Belt
307 rocks, plus the Slate Belt (Mergui Group) and all granites east of the Sagaing
308 fault and west of the Paung Laung-Mawchi Zone, as the *Mogok-Mandalay-*
309 *Mergui Belt* (MMM Belt).

310 The fourth province, the *Shan Plateau* in eastern Myanmar,
311 consists of Cambrian-Ordovician sedimentary sequences with localized
312 Ordovician volcanic rocks and volcaniclastics (Aye Ko Aung, 2012),
313 unconformably overlain by thick Middle-Upper Permian limestone sequences.
314 These latter sequences may represent the protolith carbonates of the high-
315 grade Mogok marbles. The boundary between the MMM Belt and the Shan
316 Plateau sequences is marked by the Shan Scarps and the Paung Laung-
317 Mawchi Fault Zone (Garson et al., 1976). However, some workers have
318 postulated the existence of a cryptic suture along this boundary. The
319 boundary has been suggested to have developed either as (a) a consequence
320 of the closure of the Neo-Tethys thrusting the Precambrian to Cambrian

Chaung Magyi Formation of the Shan Plateau sequences over the Slate Belt (the so-called “Medial Suture Zone” of Mitchell et al. (2015)) or (b) a major strike-slip fault (Ridd, 2016), marking the boundary of the “Phuket-Slate Belt Terrane” of Ridd and Watkinson (2013). Although the existence of such a suture would have major implications for the western extent of the Sibumasu basement (Section 5.2.1), it is nevertheless likely that continued crustal shortening and basin closure up to Late Cretaceous times (Mitchell et al., 2015), were responsible for juxtaposing the Shan Plateau and the MMM belt, resulting in the formation of contiguous basement during the Cenozoic.

3. U-Pb Geochronology

We collected several samples of magmatic rocks for zircon U-Pb geochronology that are relevant to some of the mineralization types discussed here (Table 1). Granite samples MY34 and MY37 were taken from quarries close to the Dawei tin district, sample MY76 from a quarry immediately north of Myeik, all within the southern MMM Belt. Sample MY-YAD is from the Yadanabon Mine, a primary and elluvial Sn mine in southern Myanmar, close to the Thai border (also within the MMM Belt).

MY106 is a sample of the Kabaing Granite, a peraluminous biotite granite intruding the Mogok Metamorphic Belt, and which is associated with localized base metal skarn-type mineralization (Tin Aung Myint et al., 2014). Sample MY145 is the diorite that hosts Cu-Au porphyry-type mineralization at Shangalon, lying within the southern part of the Wuntho Batholith in the WPA.

3.1. Method

Zircons grains from all samples were separated using a combination of heavy liquid and Frantz magnetic separation techniques. Selected zircons were then mounted in epoxy and imaged using a FEI Quanta 650 FEG Scanning Electron Microscope at the Department of Earth Sciences, University of Oxford.

All samples except MY106 were analyzed using the large geometry CAMECA IMS1280 ion microprobe at the NordSIM Facility housed at the Swedish Museum of Natural History, Stockholm, Sweden, using methods similar to those described by Whitehouse and Kamber (2005) and Whitehouse et al. (1999). MY106 was analyzed at the NERC Isotope Geosciences Laboratory, Keyworth, UK (NIGL), using a Nu Instruments Attom single-collector ICP-MS coupled to a New Wave Research 193UC excimer laser ablation system. The full method is described in Spencer et al. (2014).

All results used Isoplot for data presentation (Ludwig, 2004). All calculated ages are $^{206}Pb/^{238}U$ ages presented at 2σ, and include propagation of analytical and systematic uncertainties. Concordia and weighted average diagrams are presented in Fig. 4. Full zircon results are detailed in Table 2.

3.2. Results

The age for most samples is determined from the intersection of a regression line through uncorrected data, which is anchored at the modern day initial-Pb value ($^{207}Pb/^{206}Pb$ = 0.83; Stacey & Kramers (1975)), and the concordia curve (Fig. 4). The composition of common Pb has been demonstrated as appropriate for the NordSIM laboratory (Kirkland et al., 2008). As the majority of data (when ^{204}Pb corrected) is near concordant, this

form of common Pb correction does not result in significant differences to the calculated ages.

3.2.1.Sample MY34

20 analyses were performed on 18 grains. Analyses uncorrected for common Pb are concordant to significantly normally discordant, principally reflecting a mixture between radiogenic and common Pb (Fig. 4A). Two data points lie to the left of regression line and yield slightly older ^{207}Pb corrected ^{238}U/^{206}Pb ages of 65.3 and 65.4 Ma (blue, Fig. 4A). These analyses are interpreted to represent xenocrystic zircon and hence date a somewhat older inherited component within the granite (Spot IDs 02 & 17). The remaining 19 analyses define one coherent group, based on their ^{238}U/^{206}Pb and Th/U ratios (0.1-1.0), for which the regression line intersects the concordia curve at 62.3 ± 0.6 Ma (MSWD 2.1), interpreted as the magmatic crystallization age of the granite (Fig. 4A).

3.2.2.Sample MY37

19 analyses were performed on 11 grains. Zircon crystals from MY37 indicate variable U concentrations. Four data points with a U concentration <500ppm have a UO_2/U ratio within the range of the standard run during the session, hence their U/Pb ratio is regarded as robust. These four analyses when fitted with a regression from a modern day common Pb value yield an intersection with the concordia curve at 69.5 ± 1.0 Ma (MSWD 1.9), interpreted to reflect magmatic crystallization of the granite (Fig. 4B). The remaining 14 data points with higher U contents have a UO_2/U ratio outside the range of the standard for the session, reflecting the difference in sputtering characteristics of the 91500 zircon standard relative to high U

zircon (e.g. matrix matching effect; Kirkland *et al.* 2008). Nonetheless, the high U content results in high counts of radiogenic Pb and we use the $^{207}Pb/^{206}Pb$ age in preference because it is not dependent on the U/Pb calibration. The weighted average ^{204}Pb corrected $^{207}Pb/^{206}Pb$ date from the high U analyses is 70 ± 13 Ma (MSWD = 2.5), which is in close accord with the age calculated from the regression through common Pb and low U zircon (Fig. 4B).

3.2.3.Sample MY76

14 analyses were performed on 10 grains. All points from sample MY76 have extreme U contents, in some cases > 35,000 ppm. These analyses are outside the UO_2/U range of the standard during the session. Hence, in order to calculate a meaningful age from this sample we use the weighted mean ^{204}Pb corrected $^{207}Pb/^{206}Pb$ age, which yields a date of 75.3 ± 7.7 Ma (MSWD 1.8), interpreted as the age of magmatic crystallization (Fig. 4C).

3.2.4.Sample MY-YAD

18 analyses were performed on 14 grains. The analyses are concordant to discordant, principally reflecting a mixture between common and radiogenic Pb. One data point lies significantly to the right of the regression line and yields a younger ^{207}Pb-corrected age, interpreted to reflect the effects of recent radiogenic-Pb loss (spot ID n5105-02; Fig. 4D). 12 data points with high (or extreme) U content >2000ppm (blue, Fig. 4D), and a UO_2/U value outside the range of the standard used for U/Pb calibration during the analytical session, are also excluded from the regression. The remaining 5 data points yield a regression from common Pb which intersects

419 the concordia curve at 50.3 ± 0.6 Ma (MSWD 1.3), interpreted as the
420 magmatic crystallization age of the granite (Fig. 4D).

421 *3.2.5.Sample MY106*

422 Sample MY 106 is a medium-grained biotite granite. 17 analyses
423 were performed. The analyses define two populations an older concordant
424 population and a younger component that reflects a mixture between
425 radiogenic and common Pb. Two data points lie significantly to the left of a
426 regression line and yield older ^{207}Pb-corrected ages of 46.2 ± 0.6 Ma and 45.3
427 ± 0.6 Ma (blue in Fig. 4E). These analyses are interpreted to reflect
428 inheritance. 2 analyses lying slightly to the right of the regression line yield
429 ^{207}Pb corrected ^{238}U/^{206}Pb ages of 15.6 ± 0.4 Ma and 15.8 ± 0.3 Ma (Spot IDs
430 4 & 6) and are interpreted to have undergone a minor amount of geologically
431 recent radiogenic-Pb loss (red in Fig. 4E). The remaining 13 data points fit a
432 regression line which intersects the concordia curve at 16.8 ± 0.5 Ma (MSWD
433 1.9), including propagation of analytical uncertainty. This is interpreted as the
434 magmatic crystallization age of the granite.

435 *3.2.6.Sample MY145*

436 Sample MY145 is a medium-grained diorite. 14 analyses were
437 performed on 10 grains. One analysis lies to the left of a regression from
438 common Pb and yields an older ^{207}Pb age of 42.5 ± 0.7 Ma (spot ID
439 n5329_08; Fig. 4F). This analysis was located on a separate grain and is
440 interpreted to reflect inheritance. The remaining 13 data points fit a regression
441 from common Pb that intersects the Concordia curve at 40.2 ± 0.2 Ma
442 (MSWD 1.03), interpreted as the magmatic crystallization age of the granite.

4. The Minerals Endowment of Myanmar

Workers have classified Myanmar's mineral deposits into a variable number of distinct metallotects, distinguished largely on the basis of either tectono-stratigraphic association, or by commodity endowment (Bender, 1983; Chhibber, 1934; Gardiner et al., 2014; Goossens, 1979; Mitchell and Htay, 2013; Myint, 1994; Soe Win and Malar Myo Myint, 1998). Here we outline nine distinct metallogenic provinces for discussion (Table 3). While collectively these do not represent an exhaustive list of Myanmar's total mineral endowment, they reflect the relevant and known set of deposit types within Myanmar that can potentially be linked to the Tethyan metallogeneic model discussed here.

4.1. Magmatic-Hydrothermal Granite and Pegmatite-Hosted Sn-W

Southern Myanmar contains extensive, world-class tin and tungsten mineralization, principally focused in a north-south trending belt that extends from east of Yangon southwards along the Myeik Archipelago (Fig. 3). Primary deposits are strongly associated with the intrusion of Late Cretaceous-Eocene granites of the MMM Belt intruding metasedimentary rocks of the Slate Belt (Chhibber, 1934; Hutchison and Taylor, 1978; Khin Zaw, 1990). Primary tin mineralization in Myanmar is found as cassiterite-hosting quartz veins and as significant pegmatites, either within the country rock, or the upper parts of the granite intrusions. The principal tin-producing area is located around the port town of Dawei (Tavoy), where ca. 50 primary deposits are located (Fig. 3). Much historical production was alluvial/elluvial, and these deposit types are particularly focused around Myeik (Mergui) in the

467 far south (Coggin Brown and Heron, 1923; Coggin Brown, 1918; UNDP,
468 1996).

469 This metallogenic province is also rich in tungsten, found
470 spatially associated with the tin mineralization commonly as wolframite, and
471 more rarely as scheelite. In some deposits tungsten contents are found to
472 exceed tin, and there appears to be a geographic zonation in Sn:W ratio (e.g.,
473 Hobson, 1940). The Mawchi Mine, located 250 km northeast of Yangon, was
474 once a globally significant tungsten mine, briefly delivering 10% of global
475 tungsten production during the interwar period (Khin Zaw and Khin Myo Thet,
476 1983).

477 Although tin-bearing granite compositions are broadly S-type
478 (Khin Zaw, 1990), there is a geographic variation in the degree of
479 differentiation (Cobbing et al., 1992; Khin Zaw, 1990; Pollard et al., 1995;
480 Sanematsu et al., 2014). Sanematsu et al. (2014) reported that relatively older
481 Late Cretaceous to Palaeocene granites to the east of the N–S striking Dawei
482 fault are more siliceous and more highly fractionated (i.e. more S-type), whilst
483 younger Palaeocene to Eocene granites to the west are less fractionated and
484 more oxidized, implying a trend towards a I-type affinities with time.

485 *4.2. Skarn-Type Au-Ag*

486 Native gold and base metal sulphide mineralization is found
487 hosted within the phlogopite-bearing amphibolite-grade marbles of the Mogok
488 Metamorphic Belt. Approximately 50 km south of Mogok lies the Shante Gold
489 District, a 500 km^2 marble-hosted gold province spatially associated with the
490 emplacement of peraluminous granites. Mineralized quartz veins intrude the

491 marbles, and host base metal (Zn+Pb) sulphides and native Au up to 5 ppm
492 (Tin Aung Myint et al., 2014).

493 The Kwinthonze Mine, near Thabeikkyin, is a marble-hosted Au-
494 base metal sulphide deposit with accessory garnet and wollastonite,
495 interpreted as a skarn-type deposit, and through spatial association
496 interpreted as related to the intrusion of the Kabaing Granite. The Kabaing
497 Granite (sample MY106) we have dated here through zircon U-Pb
498 geochronology to ca. 17 Ma (Tin Aung Myint et al., 2014), providing some age
499 constraint on this mineralization, and interpreted as related to the late stages
500 of Mogok metamorphism.

501 *4.3. Porphyry-Type Cu-Au*

502 Within the WPA base metal (Cu) sulphide and Au deposits have
503 been documented since at least since the 1930s (e.g., Chhibber, 1934). Two
504 principal types of deposits have been found within the WPA: porphyry Cu-Au
505 and high-sulphidation epithermal-polymetallic (Au-Cu) styles (UNDP, 1996).

506 Near Wuntho, porphyry-style Cu-Au deposits occur, notably at
507 Shangalon in the south of the massif (Fig. 3). Mineralization is intimately
508 associated with magmatic intrusions (Hammarstrom et al., 2010; Mitchell et
509 al., 1999; UNDP, 1996). The main Wuntho granodiorite batholith has been
510 dated through U-Pb zircon geochronology to the Cretaceous (ca. 95 Ma)
511 (Barley et al., 2003; Mitchell et al., 2012). However, mineralization at
512 Shangalon is spatially associated with the Eocene intrusion of finer-grained
513 micro diorite into the hosting batholith. The hosting diorite is here dated using
514 U-Pb in zircon geochronology at 39.9±0.31 Ma (sample MY145), providing a
515 reasonable estimate for the age of mineralization. Porphyry-type

516 mineralization has been reported elsewhere in the Wuntho area (Goossens,
517 1979; UNDP, 1978), but have no definitive age constraints.

518 *4.4. Epithermal Au-Cu*

519 Epithermal Au-Cu mineralization has been recognized at several
520 localities within the WPA (Goossens, 1979; UNDP, 1996). Auriferous quartz
521 veins have been reported near Wuntho. They are hosted both by the
522 granodiorite and diorite magmatic rocks, and by the country rocks, and
523 mineralization has been interpreted as being at latest of Cretaceous age
524 (Mitchell et al., 1999). However, geochronology suggests that some
525 epithermal-type deposits in the WPA may be of Miocene-age. The Monywa
526 Cu Mine further south, which includes the giant Leptadaung deposit, has been
527 interpreted as a high-sulphidation epithermal deposit, and is characterized by
528 the absence of economic-grade Au (Mitchell et al., 2011). The same workers
529 inferred an age of formation for Monywa of mid-Miocene on the basis of U-Pb
530 radiometric age dating of a local dyke.

531 Historically, most Au production in the northern WPA region has
532 been from high-grade auriferous quartz veins, found both in the granodiorites
533 and surrounding host rocks, and from derived placers in the northerly Wuntho
534 and Tagaung-Myitkyina segments of the WPA (Chhibber 1934; Mitchell et al,
535 1999).

536 *4.5. Ultramafic-hosted*

537 Ultramafic-hosted deposits within Myanmar are focused around
538 the various ophiolite fragments found within the country. The poorly-studied
539 Tagaung-Myitkyina Belt (TMB) lies between the Mogok Metamorphic Belt and
540 the Katha-Gangaw Belt (KGB) in the north of the country (Fig. 3). Outcropping

541 along the eastern bank of the Irrawaddy River in the Kyawbingyon Region, the
542 TMB comprises significant ophiolitic mantle peridotite (Searle et al., 2016).
543 Extreme weathering of these TMB ultramafic rocks has resulted in lateritic
544 deposits rich in nickel. The large Tagaung Taung Mine, 200 km north of
545 Mandalay, is a major nickel laterite deposit that was discovered by BGR
546 geologists in the early 1980s. At Tagaung Taung the laterites are associated
547 with outcrops of precursor dunite, harzburgite and serpentinite (Schellmann,
548 1989).

549 The Jade Mines Belt (JMB, Fig. 3), another metamorphic belt,
550 lies along the northern segments of the Sagaing Fault. The Jade Belt is a
551 high-P subduction-related assemblage (Goffe et al., 2002). Although
552 dominated by outcrops of peridotite and serpentinite, it remains poorly
553 exposed and little studied. The majority of mined jade is sourced from
554 bounders in young alluvial deposits along the Uru River (e.g., Hughes et al.,
555 2000). A variety of jade rock assemblages have been reported: pure jadeitite,
556 amphibole jadeite, omphacite-jadeite-zoisite-kyanite and kosmochlor (Franz et
557 al., 2014; Goffe et al., 2002). The Hpakant region is globally unique in the
558 extensive occurrence of pure jade, jadeite (Hughes et al., 2000).

559 Chromite and nickel deposits have been recognized in the
560 ultramafic rocks of the Western Ophiolite Belt (Section 5.3) within in the Chin
561 and Naga Hills (Bender, 1983; Chhibber, 1934).

562 *4.6. Orogenic-Type Au*

563 Gold mineralization has been recognised at numerous localities
564 throughout the Slate Belt (e.g., Bender, 1983; Mitchell et al., 1999; Zaw Naing
565 Oo and Khin Zaw, 2009). Although neither its genesis nor age is well

566 constrained, workers have inferred the mineralization to be of Orogenic type
567 (Khin Zaw et al., 2014; Mitchell et al., 2004). Several deposits have been
568 studied. The Meyon gold deposit in southern Myanmar is interpreted as
569 structurally controlled, and related to movement on the Papun Fault Zone
570 (Zaw Naing Oo and Khin Zaw, 2009). The same workers bracketed the age of
571 mineralization as Late Cretaceous to Palaeogene.

572 However, the most detailed study to date of this mineralization
573 style in Myanmar has been undertaken at the Modi Taung-Nankwe Gold
574 District in central Myanmar, where Au mineralization is associated with quartz-
575 pyrite stringers and veinlets cutting the Slate Belt. Mitchell et al. (2004)
576 suggested that at Modi Taung, gold mineralization was related to the ascent
577 of metamorphic fluids following prograde metamorphism of the Mogok
578 Metamorphic Belt, which they inferred to be of Jurassic Age, but which has
579 since been dated by monazite U-Pb geochronology as Eocene-Oligocene in
580 age (Searle et al., 2007). However, older age constraints on Slate Belt gold
581 mineralization have been proposed, discussed in Section 6.2.3.

582 *4.7. Sediment-hosted Pb+Zn Sulphide Deposits*

583 Several significant carbonate-hosted Pb-Zn sulphide deposits
584 have been reported from the Upper Palaeozoic carbonate sequences of the
585 Shan Plateau. The Theingon (or Bawsaing) Pb+Zn+Ag Mine in the Southern
586 Shan States has been interpreted as a stratabound carbonate-hosted
587 Mississippi Valley Type (MVT) or Irish type deposit of Ordovician age(Khin
588 Zaw et al., 2014, 1984).

589 *4.8. Gemstones*

590 Arguably the World's finest rubies are sourced from the stone
591 tracts of Mogok in central Myanmar, hosted by the metamorphic rocks of the
592 Mogok Metamorphic Belt. Gem-quality rubies are derived from corundum ±
593 phlogopite ± clinopyroxene ± forsterite ± spinel-bearing marbles both around
594 Mogok, and north of Mandalay; sapphires are found in spatial association with
595 nepheline syenites that intrude these marbles (Bender, 1983; Chhibber, 1934;
596 Iyer, 1953; Mitchell et al., 2007; Searle and Ba Than Haq, 1964; Searle et al.,
597 2007; Themelis, 2008).

598 Gem rubies are thought to form through the thermal reduction of
599 evaporites during high temperature, medium pressure metamorphism of
600 platform carbonates (Garnier et al., 2008). The evaporite sequences contain
601 sufficient trace element contents of Al and Cr derived from entrained clay
602 material to produce ruby, a form of corundum. Some workers have interpreted
603 Mogok sapphires as the products of assimilated, partially melted lower crustal
604 material formed during intrusion of the syenites into the Mogok Metamorphic
605 Belt (Searle et al., 2016). Topaz, tourmaline and aquamarine (beryl) are
606 mined from pegmatite dykes that are associated with the Kabaing Granite that
607 intrudes the marbles immediately west of Mogok town (e.g., Iyer, 1953),
608 whereas gem-quality spinels are also found in forsterite-bearing marbles. All
609 these gemstones have withstood the processes of extreme lateritization, and
610 are now largely found in outcrop and enclosed in tropical red soils known
611 locally as *byons* from which they are mined.

612 Age determinations of both pelites, and from metasomatic rubies
613 found in the marbles, has led to the interpretation of two peak amphibolite-

614 grade Mogok metamorphic events – one occurring in the Palaeocene and the
615 other during the Eocene-Oligocene (Khin Zaw et al. (2010) reported in
616 Mitchell et al., 2012; Searle et al., 2007). $^{40-39}$Ar cooling ages from phlogopite
617 found in the Mogok marbles have yielded Miocene ages (18.7-17.1 Ma;
618 Garnier et al., 2006), interpreted as the date of ruby formation. This would
619 imply that ruby formation occurred during an Early Miocene retrograde phase
620 following peak amphibolite-grade Eocene-Oligocene metamorphism. This is
621 also similar to our magmatic age for the Kabaing granite, the intrusion of
622 which led to pegmatite-hosted topaz and aquamarine.

623 *4.9. Sediment-hosted Epithermal Au*

624 The largest gold-producing mine in Myanmar is the Kyaukpahto
625 Mine, sited in Kawlin Township, Sagaing Division. Au mineralization is
626 associated with stockwork-style quartz veins hosted in silicified sandstones,
627 and formed during extensional faulting. Veins comprising pyrite, chalcopyrite
628 and arsenopyrite (Ye Myint Swe et al., 2004) are best developed in competent
629 silicified sandstone locally extending into the adjacent mudstones of the
630 Lower-Mid Eocene Male Formation (Mitchell et al., 1999). These host rocks
631 have undergone intense hydrothermal alteration and silicification, which
632 appears to be critical for the genesis of the veining, the latter generally
633 confined to the silicified sandstone.

634 Fluid circulation and vein formation is most probably related to
635 movement on the Sagaing Fault. NNE-trending extensional faults formed by a
636 component of dextral strike-slip movement host the stockwork epithermal Au
637 mineralisation structures (Ye Myint Swe et al., 2004).

5. Tectonic Model

We propose a Late Mesozoic-Cenozoic tectonic model that provides a framework for the discussion of metallogenesis. Key aspects for discussion are (a) the age and tectonic relationships between the two magmatic belts, and (b) the nature and continuity of the underlying crust.

5.1. Age of Magmatic Belts

Geochronology suggests that at least two main magmatic episodes occurred within the WPA, which were followed by a Quaternary episode of andesite-dacite stratovolcanoes related either to subduction-related magmatism (Stephenson and Marshall, 1984) or slab detachment and asthenospheric upwelling (e.g., Maury et al., 2004). U-Pb geochronology from magmatic zircon analysis suggests (a) a short period of magmatism operating in the Mid-Late Cretaceous (Barley et al., 2003; Mitchell et al., 2012); (b) a magmatic Eocene event (Shangalon; our new data and similar reported in Barley *et al.* 2003); and (c) activity in Miocene times (Mitchell *et al.* 2012).

Excluding the most recent event, are we dealing with three separate magmatic episodes, or was the magmatism continuous but not reflected in the few age data available? Detrital zircon ages from Cretaceous to Miocene successions in the Chindwin Basin, the forearc of the Wuntho-Popa Arc, were reported by (Wang et al., 2014). Interpreting these to have WPA provenance, Wang et al. (2014) suggested their data implied a main magmatic stage for the Arc of between 110-80 Ma, and a lesser subordinate stage between 70-40 Ma. Our new age for Shangalon lies within the younger of these. Therefore, it is possible the Arc was near-continuous from the Mid-

662 Cretaceous to Eocene times, and then experienced a late Miocene event
663 during which the Monywa deposit formed.

664 U-Pb ages from the MMM Belt indicate earlier Jurassic and
665 Triassic Indosinian-related magmatism (ca. 170 Ma; Barley et al., 2003); an
666 extended period of Cretaceous to Eocene magmatism (e.g., Aung Zaw Myint
667 et al., 2016; Mitchell et al., 2012; Sanematsu et al., 2014; our new data); and
668 leucogranites and other magmatism associated with Oligocene-Miocene
669 metamorphism (e.g., Searle et al., 2007; our Kabaing Granite data). MMM
670 Belt granites evident a general trend towards more S-type affinity with time
671 (Cobbing et al., 1992). This change in magmatic style with time is perhaps
672 related to slab rollback in a continental subduction or island arc setting (e.g.,
673 Mitchell, 1986; Mitchell and Myint Thein Htay, 2013; Sanematsu et al., 2014).

674 The recognition that the WPA and MMM Belt are sub-parallel
675 magmatic belts hosting contrasting mineralization styles (Cu-Au and Sn-W
676 respectively) prompted the consideration of their tectonic and metallogenic
677 implication as a pair (full review in Gardiner et al., 2015b). Mitchell (1979)
678 noted a similarity with the metallogenic belts of the South American Cordillera
679 (Peru/Bolivia). In this analogue, the WPA would represent the intrusion of
680 subduction-related I-type magmatism sited immediately above the plate
681 margin, associated with porphyry and epithermal-type Cu-Au mineralisation
682 (Fig. 5A). Thus the WPA is analogous to the coastal copper belts of the
683 Central Andes. Conversely, the Cenozoic intrusions of the MMM Belt results
684 from magmatism sited more distally to the plate margin, being sourced from
685 the melting of more reduced, dominantly pelitic protoliths, and giving rise to
686 crustal-melt S-type granites and associated lithophile tin-tungsten

687 mineralization (Fig. 5A). The MMM Belt would therefore find a geodynamic
688 parallel in the Bolivian tin belts, at least with commodity type, if not
689 mineralization style *per se*.

690 Although there is some evidence for contemporary magmatism
691 in the Eocene, the various styles of mineralization between and within these
692 belts are potentially of different ages. Further, the relationship between the
693 higher grade Mogok Metamorphic Belt containing both older and much
694 younger magmatism, and the early Cenozoic magmatism in the Slate Belt is
695 unclear. Despite these issues, we believe a case may still be made that the
696 WPA and certainly the southern Slate Belt part of the MMM may represent
697 paired magmatic belts. If so, then a tectonic setting for their petrogenesis is
698 perhaps an Andean-type accretionary setting on the margins of a subducting
699 Neo-Tethys during the Late Cretaceous-Eocene prior to the collision of India
700 (Gardiner et al., 2015b; Mitchell, 1979). We take this framework for the
701 ensuing discussion.

702 *5.2. The Crustal Evolution of Myanmar*

703 The western extent of Sibumasu is uncertain. Some workers
704 have proposed the existence of an intermediate ocean basin, the so-called
705 Meso-Tethys, that may have separated the MMM Belt from the Shan Plateau.
706 The nature of the crust underlying western Myanmar, including the WPA, has
707 been the subject of recent study. Defining a feasible tectonic model for
708 Myanmar during the Late Mesozoic-Cenozoic requires addressing these two
709 issues.

710 *5.2.1.A Thai-Myanmar Meso-Tethys Suture?*

711 The existence of a Meso-Tethys within the area typically defined
712 as Sibumasu has received recent attention in the literature (Mitchell et al.,
713 2015, 2012; Ridd, 2015), and which has been proposed several times
714 previously (Cooper et al., 1989; Mitchell, 1992). In Yunnan, a proposed Meso-
715 Tethys suture (Nujiang suture) forms the boundary between the Tengchong
716 and Baoshan Blocks (see review in Burchfiel and Chen Zhiliang (2013)). One
717 of the key differences between the blocks relates to the Palaeozoic
718 stratigraphic column, in particular the thick (1000's m), well-developed nature
719 of Carboniferous-Early Permian glacio-marine sediments on the Tengchong
720 Block, and much less well developed nature of equivalent sediments (10's-
721 100's m thick) in the Baoshan Block. The question is whether these
722 stratigraphic differences can be explained by variations within a single
723 continental block, such as thickness changes due to rifting (e.g., Ridd, 2009),
724 or whether an ocean basin once separated the blocks. The Nujiang suture is
725 largely cryptic due to overprinting by Himalayan deformation (Burchfiel and
726 Chen Zhiliang, 2013). In Yunnan and Tibet the Baoshan Block is considered
727 to be equivalent to the South Qiangtang Block, while the Tengchong Block is
728 equivalent to the Lhasa Block, and in these areas there is clear evidence for a
729 major ocean based on abundant arc volcanic rocks, ophiolitic remnants, and
730 palaeomagnetic evidence for up to 31° of latitudinal separation between the
731 Lhasa and Qiangtang blocks (Otofuji et al., 2007). Even in the better-known
732 parts of the Nujiang suture the timing of closure is uncertain, with some
733 arguing for an Early Cretaceous closure at around 120 Ma (Cao et al., 2014;
734 Chen et al., 2004; Raterman et al., 2014; Zhao et al., 2015; Zhu et al., 2015,

735 2012) and others preferring a Late Cretaceous closure (Fan et al., 2015;
736 Wang et al., 2015).

737 Similar stratigraphic characteristics as those defining the
738 Tengchong and Baoshan Blocks are present along a line that runs along the
739 Paung Laung Fault in Myanmar, the Three Pagodas and Khlong Marui faults
740 in Thailand, and the Straits of Malacca between Malaysia and Sumatra
741 (Mitchell et al., 2015, 2012; Ridd, 2015). Ridd (2015) refers to the western
742 area (western Myanmar, northern Peninsular Thailand and Sumatra) as the
743 Irrawaddy Block, and the eastern area as Sibuma. Stratigraphically, the
744 argument seems as compelling as in Yunnan, but structurally and tectonically
745 evidence for a suture is not strong, perhaps because of overprinting by later
746 thrusting and strike-slip motion (Ridd, 2015). Here we accept that a significant
747 oceanic-floored rift relating to the Meso-Tethys at least partially if not
748 completely separated Sibumasu into two separate blocks, which nevertheless
749 seems likely to have sutured by the Late Cretaceous.

750 *5.2.2.The West Burma Plate*

751 The tectonic units to the west of the Shan Plateau have been
752 subject to numerous interpretations. Much discussion has focused around the
753 existence or otherwise of a separate microplate, variously described as the
754 Burma Plate, Burma Platelet, West Myanmar Terrane, or most commonly as
755 the *West Burma Block* (Curray, 2005; Curray et al., 1979; Metcalfe, 2011;
756 Rangin et al., 2013). This block has been separately invoked as (a) explaining
757 the S-type, tin-bearing granitic plutons of the MMM Belt (Charusiri et al., 1993;
758 Hutchison, 1994); and/or (b) explaining Palaeogene deformation in the Indo-
759 Burma Ranges (Acharyya, 2010, 2007). Its origin has also been explained as

760 due to (a) Early Carboniferous accretion onto South China as part of
761 Indochina, followed by strike-slip emplacement onto the western margin of
762 Sibumasu during the mid-Cretaceous (Barber and Crow, 2009); (b) as Late
763 Cenozoic as a result of hyper-oblique convergence, forming the region
764 between the Sunda Trench and the Sagaing-Sumatra fault systems (Rangin
765 et al., 2013); or (c) only established in the Mid-Eocene as a consequence of
766 movement along the Sagaing Fault, thereby dividing Sibumasu (Mitchell,
767 1993).

768 Assuming the West Burma Plate was a separate block,
769 Sevastjanova et al. (2015) undertook detrital U-Pb zircon age analyses from
770 Triassic turbidite sandstones locally overlain by pillow basalts, within the Chin
771 Hills in western Myanmar (Fig. 3). They found evidence of Permian-Triassic
772 magmatism, interpreted as being sourced from the Palaeo-Tethys related
773 granite belts further east. They also identified chromium spinels, which are
774 common in Southeast Asia but rare in an Australia lacking significant ophiolitic
775 material, the likely source of this block. They concluded that both West Burma
776 and Sibumasu together formed part of Gondwana at least until the Devonian,
777 and that the West Burma Plate had most likely docked onto Southeast Asia
778 before Mesozoic times.

779 Isotopic analysis of detrital zircons sourced from the Cretaceous-
780 Miocene successions of the Chindwin Basin, thought to represent the forearc
781 of the WPA, were reported by Wang et al. (2014). Zircon Hf signatures of
782 samples with a Cretaceous-Eocene magmatic-age yielded largely radiogenic
783 εHf values, corresponding to two stage model ages of 1.0-1.2 Ga, and
784 suggestive of a more juvenile source for WPA magmas. Reported εHf data

785 from eastern Sibumasu sampled in Thailand and eastern Myanmar have
786 yielded εHf values in the range of +3.7 to – 10.5, representing Meso- to
787 Palaeoproterozoic model ages (Gardiner et al., 2015a; Lin et al., 2013).
788 We suggest that these data indicate that the West Burma Block
789 may be an artifact of movement on the Sagaing Fault, and that the continental
790 crust underlying western Myanmar is either Sibumasu crust, or a separate
791 block accreted possibly by the mid-Cretaceous at the latest. This scenario
792 allows both magmatic belts (the WPA and the MMM Belt) to have formed as
793 adjacent parallel belts on a common continental margin, overlying the
794 subducting Neo-Tethys.

795 *5.3. Ophiolite Belts*

796 Reconstruction of the Late Mesozoic-Cenozoic history of
797 collision in Myanmar is largely dependent on interpretation of the various
798 ophiolite fragments. Ophiolite outcrops in Myanmar are thought to comprise at
799 least two distinct belts (Hutchison, 1975; Mitchell, 1993). The *Western Belt*
800 (WB in Fig. 1) follows the trend of the eastern Indo-Burman Ranges, and is
801 best described from the Naga Ophiolite (Acharyya, 2010, 2007). This belt has
802 been interpreted to represent the final closure of the Neo-Tethys during the
803 late Eocene (Acharyya, 2007; Ghose et al., 2014), being the eastern suture of
804 the Indian Plate. The *Eastern Belt* (EB in Fig. 1) lies east of the Indo-Burman
805 Ranges as fragments in both the Jade Mines Belt and in the Tagaung-
806 Myitkyina Belt, and may include ophiolite fragments found within the Mount
807 Victoria Belt (Acharyya, 2007; Mitchell, 1993; Mitchell et al., 2011). The
808 Eastern Belt has been interpreted by some to represent the earlier closure of
809 a back-arc ocean between either a continental block (e.g., Acharyya, 2010),

or an accreted volcanic arc (i.e. the Mawgyi Nappe of Mitchell (1993), and Southeast Asia.

Neither the age of oceanic crust formation, nor the timing of obduction and/or emplacement, of any of the ophiolite fragments found within Myanmar are precisely known. Some workers have placed the Western Belt ophiolites as Jurassic in age (Suzuki et al., 2004). Working in the Naga Hills, within the Western Ophiolite Belt, Ghose et al. (2014) used stratigraphic associations to infer the timing of final emplacement of the Naga Ophiolite as Eocene, although this age may reflect a later thrusting event and not the original emplacement event. A recent study by Yui et al. (2013) on zircon populations from two jadeitite samples from the Jade Mines Belt (Hpakant area), in the Eastern Ophiolite Belt, yielded Jurassic ages from the older zircon age population. However these were sourced from inherited or incompletely recrystallized and fractured zircon grains, such that their apparent mineral inclusions, e.g., jadeite, are not necessarily as old as the determined ages. However, Yui et al. (2013) reported a chemically distinct group of zircons that showed a typical metasomatic-hydrothermal signature, and which gave a Cretaceous U-Pb age of 77±3 Ma. This is consistent with jadeitite formation through the flux of Na-rich metasomatic fluids during Late Cretaceous subduction, an age supported by $^{39\text{-}40}$Ar dating of phengites by Goffe et al. (2002) that gave a large age spread of 80-30 Ma. It is therefore possible that the protolith of these Hpakant jadeitites, and thus of the Jade Mines Belt, may have been older components of a Jurassic ophiolitic suite, but that metasomatic conversion of precursor ophiolite to jadetite was Late Cretaceous in age.

Mitchell (1993) proposed that the Eastern Ophiolite Belt represents a truncated northerly extension of the Western Ophiolite Belt, which has been offset southwards by movement on the Sagaing Fault. Given modern-day slip rates, such a displacement would require ca. 450 km of fault movement, which necessitates a longer-lived fault than is currently interpreted by some workers, specifically one stretching back to the Miocene. Delineating a single ophiolite belt simplifies Myanmar's geological history east of the Shan Scarps by requiring the closure of a single ocean basin: Neo-Tethys. Further, this also removes the requirement for a separate West Burma Plate (e.g. Curray et al., 1979) during the late Mesozoic and early Cenozoic, supporting the view of Mitchell (1993) that the West Burma Plate is an artifact of later movement on the Sagaing Fault. This scenario accommodates the concept of a continuous basement extending under Myanmar as far west as the continental margin in the Cenozoic, with the implication that Mesozoic ophiolites were obducted before or during the Cretaceous onto the Burma Plate (e.g., Searle et al., 2016) and were subsequently subducted under high pressure, before being exhumed during collision, and then finally offset by dextral shearing along the Sagaing Fault.

6. Tethyan Metallogenesis

In line with the tectonic evolution described above, we propose a simplified orogenic model for the Mesozoic-Cenozoic geological evolution of Myanmar: an accretionary margin on the western edge of Asia, sited above the easterly subduction of the Neo-Tethys, and operating from at least the Late Cretaceous to Eocene times. Suturing of the Neo-Tethys likely occurred in the mid-late Eocene, and the ensuing Himalayan Orogeny caused

concomitant crustal thickening that continued to at least the Oligocene. Ongoing rotation around the Eastern Syntaxis forced plate convergence, likely oblique at inception, to become increasingly hyper-oblique, eventually initiating movement on the Sagaing Fault, possibly as early as the Miocene, becoming a major transform boundary seen today.

6.1. Metallogenic-Tectonic Model

Mineral deposits form under specific conditions within specific tectonic and geodynamic settings (Barley and Groves, 1992; Bierlein et al., 2009; Groves and Bierlein, 2007; Kerrich et al., 2005; Mitchell and Garson, 1981). The Tethyan collision zone, resulting in the Alpine-Himalayan Orogeny, has, in places, proved a highly fertile zone for metallogenesis (e.g. review in Richards, 2014). We define four major stages of orogenic evolution in our model of the Himalayan Orogeny in Myanmar, outlined in Fig. 6. Each of these describes a specific temporally-constrained geodynamic setting as follows:

(a) *accretionary* (100-50 Ma)

(b) *collisional* (50-30 Ma)

(c) *late collisional* (30-20 Ma)

(d) *highly-oblique collisional* (15-0 Ma).

Although we define only the final stage as being oblique, we accept that the collision was likely oblique to a significant degree for much of its history. To this tectonic framework, we assign the nine major deposit types described in Section 0 on the basis of either age constraints (inferred or measured), or from geological observations that lead to an interpreted

884 tectonic setting for its genesis. Fig. 5 shows the schematic genesis for a
885 number of these metallotects.

886 *6.1.1.Accretionary Stage (100–50 Ma)*

887 An Andean-type accretionary setting on the margins of the Neo-
888 Tethys operated in central Myanmar from the Late Cretaceous to Eocene.
889 This setting was responsible for the generation of extensive subduction-
890 related I-type magmatism, which was principally focused in the WPA.

891 Tin-tungsten mineralization is located where granites of the
892 MMM Belt intrude the Slate Belt (e.g. at Hermyingyi, Mawchi and
893 Yadanabon). Zircon U-Pb studies indicate crystallization ages of both
894 mineralized and presumed coeval non-mineralized granites within the MMM
895 Belt are largely of Palaeogene age. Our zircon U-Pb ages of 75–50 Ma
896 (MY34, MY37, MY76, and MY-YAD) from granites within the southern MMM
897 belt that are either within the Dawei vicinity and thus potentially coeval with
898 mineralized granites, or sample a mineralized granite (MY-YAD), compare
899 favourably with previously published geochronological data of magmatism in
900 the range of 70-50 Ma (Barley and Khin Zaw, 2009; Sanematsu et al., 2014).

901 *6.1.2.Collisional Stage (50-30 Ma)*

902 Closure of the Neo-Tethys marks the transition from an
903 accretionary to a continent-continent collisional setting and the onset of
904 crustal thickening. Before or during this period, emplacement of Tethyan
905 oceanic material onto the continental margins occurred. This ophiolitic
906 material is responsible for deposits of podiform chromite, jade and nickel.
907 Jade (jadeite) results from subduction-zone high P metasomatic
908 metamorphism of oceanic lithosphere (e.g., Stern and Scholl, 2010), which in

909 Myanmar possibly occurred during the Late Cretaceous (Section 5.3). Nickel
910 laterite deposits (e.g. Tagaung Taung; Schellmann, 1989) result from later
911 supergene reworking of ultramafics.

912 Ongoing orogeny and enhanced crustal thickening drove
913 metamorphism and anatexis. This protracted metamorphic event was also
914 responsible for the formation of the marble-hosted gemstones found at
915 Mogok; namely ruby, sapphire and spinel (Searle et al., 2016). In Myanmar, it
916 is possible that the deep amphibolite-grade metamorphism resulted in the
917 release of scavenging fluids and the subsequent development of the orogenic
918 Au deposits although this is subjective and is discussed below.

919 During this period the Eocene diorite that hosts the Shangalon
920 Mine was intruded, which we suggest provides a best estimate for the
921 porphyry-type mineralization observed here.

922 *6.1.3.Late Collisional Stage (30-20 Ma)*

923 Geochronology suggests a Miocene-age, period of WPA activity
924 during this period, responsible for the development of the Monywa Cu
925 epithermal deposit. Late-stage magmatism is associated with the
926 development of skarn-type deposits within the high-T marbles of the Mogok
927 Metamorphic Belt.

928 *6.1.4.Highly-Oblique Collisional Stage (15-0 Ma)*

929 The continuing northwards movement of the Indian Plate drove
930 the clockwise rotation of terranes around the syntaxis during Oligocene-
931 Miocene times, and initiated movement on the strike-slip Sagaing Fault.
932 Faulting is interpreted to have helped drive sandstone-hosted low-sulphidation
933 epithermal Au mineralization, driven by circulation of auriferous hydrothermal

fluids, and occurring as vein stockworks in small pull-apart basins (example of Kyaukpahto; Ye Myint Swe et al., 2004). Fig. 5C shows a schematic genesis for such seismically-pumped gold deposits.

6.2. Discussion of Model

In Myanmar, limited zircon U-Pb geochronology has yielded the magmatic ages of granites. According to metallogenetic interpretations, these ages can inform on the age of mineralization of granite-hosted ore deposits. However, a number of mineralization styles presented here lack firm age constraints. In our model we therefore derived proposed ages of their geneses on the basis of inferred tectonic settings, and below we discuss the evidence and limitations for placing these less well-constrained deposits into our metallogenic framework.

6.2.1.Age of Magmatic-Hydrothermal Tin-Tungsten deposits

There are limited age constraints on the crystallization ages of tin-hosting granites, and even less work on constraining the actual age of mineralization. In general, tin-tungsten mineralization appears to be spatially associated with Palaeogene S-type granites, and major deposits whose crystallization age has been constrained through zircon U-Pb geochronology include Hermyingyi (62 Ma; Barley and Khin Zaw, 2009), Mawchi (45-43 Ma; Aung Zaw Myint et al., 2016), and Yadanabon (51 Ma, our new data). We suggest that the age of mineralization of these southern Myanmar tin granites is best estimated from the magmatic crystallization ages.

6.2.2.Age of Porphyry and Epithermal Deposits

Geochronology from the WPA records at least two major epochs of magmatic activity: Late Cretaceous to Eocene and late Cenozoic. The only

two definitively dated deposits are Eocene (Shangalon; MY145 age data presented here) and Miocene (Monywa) (Mitchell et al., 2011). There have been no reported ages of either porphyry-type or epithermal mineralization from the late Mesozoic despite this being the timing of the main batholith intrusions. This may be due to a lack of analyses, poor preservation potential of such high-level deposits, or simply that no mineralization occurred during this earlier magmatic event.

6.2.3.Orogenic Gold

The age and origin of the quartz-hosted gold mineralization found within the Slate Belt is not well constrained. Despite the presence of local granite intrusions, mineralization is not spatially related to these granites. Mitchell et al. (2004), in their study of Modi Taung, inferred it to be of orogenic style, linking its genesis with migrating fluids liberated during metamorphism of the Mogok Metamorphic Belt. They interpreted this metamorphism to be Jurassic in age, thus inferring this age for the mineralization, although Searle et al. (2007) have proposed a much younger Palaeogene age for peak Mogok metamorphism. Mitchell et al. (2004), on the basis of cross-cutting evidence considered that the orogenic gold-hosting quartz veins were emplaced prior to granite magmatism. Zircon LA-ICP-MS U-Pb dating of dykes that intrude the mineralization have yielded an age of 49 ± 1 Ma (Eskine et al., 2015), providing a lower age boundary.

Globally, orogenic gold deposits are typically associated with the waning stages of orogenic compression and metamorphism. Mineralization results from the release of fluids during regional metamorphism which then migrate to higher levels in the mid-crust, and occurs in rocks of amphibolite to

greenschist facies grades (Bierlein and Crowe, 2000; Goldfarb and Groves, 2015; Goldfarb et al., 2005; Groves et al., 1998). Orogenic gold deposits are found both within pre-collisional accretionary margins, and post-collisional orogenic belts. Fig. 5B shows a schematic for the genesis of Myanmar's Slate Belt Orogenic gold.

At least two major orogenic events have affected Myanmar during the Mesozoic-Cenozoic, and which could be candidates for causing widespread regional metamorphism and therefore driving the Slate Belt gold mineralization. The Indosinian Orogeny has an inferred suture zone some 100-300 km west in present day terms, and linking such a relatively distal orogenic event to the gold mineralization requires the closure of any intermediate ocean basin (e.g., Meso-Tethys) by Late Triassic times, the age of Palaeo-Tethyan suturing. If the Au mineralization were related to the closure of the Neo-Tethys, the 49 Ma age of dyke intrusion as reported by Eskine et al. (2015), does not preclude it to be related to the Eocene onset of the Himalayan Orogeny. The timing thus remains equivocal.

6.2.4.Sediment-hosted Pb-Zn sulphide deposits

Sediment-hosted deposits have a genesis related to the circulation of low-temperature brines usually in response to far-field orogenic events (Leach et al., 2005), and hosted in carbonate platforms of marginal or shelf origins. Proposed fluid drivers in such settings include a combination of orogenic uplift (gravity)–driven groundwater and tectonic-driven dewatering.

However, no definitive ages have been published thus far to this style of mineralization in Myanmar, although their hosting Lower Palaeozoic sequences provide a maximum age bracket. One MVT-type deposit within

1009 Sibumasu has been interpreted as directly related to Cretaceous-era orogeny.
1010 Mineralization in the vicinity of Mae Sod in Thailand was interpreted to be
1011 have developed in response to Cretaceous uplift and deformation on the
1012 western margin of Sibumasu (Reynolds et al., 2003). The economic-grade
1013 non-sulphide Padaeng Zn deposit was interpreted by the same authors to
1014 have formed by later supergene enrichment of these local MVT deposits.

1015 **7. A Tethyan Mineral System?**

1016 An orogenic system is a highly fertile regime for the provision of
1017 the geologic factors (e.g., structures, fluids, transient geodynamic trigger) that
1018 promote the generation and preservation of mineral deposits, as evidenced by
1019 the variety of deposits found associated with such settings (e.g., Cawood and
1020 Hawkesworth, 2013; Groves and Bierlein, 2007; Kerrich et al., 2005).
1021 Orogenic belts accommodate the genesis of multiple types of magmatism,
1022 and the gestation of fluids of varying compositions through elevated P-T
1023 conditions and metamorphic dehydration reactions. Furthermore, the dynamic
1024 nature of the orogenic system gives rise to a changing lithospheric
1025 architecture with evolving conduits for metalliferous fluids, widely dispersed at
1026 low concentration, to localize in high concentrations (McCuaig and Hronsky,
1027 2014). Mineral deposits are thus commonly clustered in geological provinces
1028 with particular areas strongly endowed in specific commodities (Arribas et al.,
1029 1995; Carlson, 1991). All these orogeny-driven metal transport processes
1030 operate on a variety of scales from continent to deposit.

1031 At the lithospheric-scales of observation described here, the
1032 identification of discrete large-scale critical geological factors that together
1033 may have influenced the formation of mineral deposits leads to a mineral

1034 systems type approach (e.g. McCuaig et al., 2010). In Myanmar, the major
1035 discrete orogen-scale factor that governs the type and distribution of mineral
1036 deposit types in Myanmar is the evolving geodynamic setting.

1037 The major geodynamic elements evolve over the lifetime of the
1038 Himalayan Orogen in Myanmar. Magmatism is the main driver of ore
1039 formation during the early to mid part of orogenic progression, acting both as
1040 a source of heat and potentially of metals of economic interest. The
1041 geodynamic configuration of an accretionary orogen is interpreted to strongly
1042 govern the geochemical nature and spatial distribution of resultant
1043 magmatism, with implications for metallogeny (Sillitoe, 1972). Arc-type
1044 magmatism sited immediately above the subduction zone through its potential
1045 for chalcophile-type (e.g., Cu, Au and Mo) mineral deposits shows a clear
1046 relationship to subduction-driven processes (e.g., Hedenquist and
1047 Lowenstern, 1994). In Myanmar this magmatism leads to the development of
1048 the WPA-hosted porphyry deposits, and fertilizes the overlying epithermal
1049 processes that operate at least during the Miocene. It is possible, although
1050 speculative, that Cretaceous-era deposits developed within the WPA, but
1051 which have since been either eroded or are not yet recognized.

1052 As this margin developed over time, the input of heat and onset
1053 of crustal thickening promoted crustal anatexis, leading to the development of
1054 melts that produced compositionally evolved crustal-melt S-type granites,
1055 most likely derived from sedimentary successions, and resulting in typically
1056 more reducing granites associated with lithophile Sn-W mineralization. After
1057 the onset of suturing in the early Eocene (ca. 50 Ma), these crustal thickening
1058 effects become increasingly dominant, driving both the generation, and the

movement, of various magmatic-hydrothermal fluids. Elevated P-T regimes in the mid-crust drive widespread regional metamorphism, producing substantial volumes of low salinity aqueo-carbonic fluids through dehydration and decarbonation reactions. These fluids migrate upwards, scavenging metals, which may lead to the formation of orogenic-style gold deposits in suitable host traps. Late-stage magmatism driven through high-T metamorphism leads to the development of skarn-type deposits in appropriate hosting rocks.

During the latter stages of orogeny in Myanmar the collision becomes increasingly oblique and in some cases trans-tensional, with major strike-slip faulting emerging as the dominant geodynamic regime. Faulting promotes the movement of low-T fluids and development of epithermal gold deposits in the brittle upper crust, hydrothermal fluid movement being driven by seismic pumping. Uplift and exhumation facilitates later, supergene alteration, leading to the development of the Ni laterite deposits (Schellmann, 1989).

7.1. Timescales of Metallogeny

Advances in the dating of geological processes have shown that many ore deposits form over a relatively short time period associated with specific geological processes. Timescales of mineral deposit genesis versus geodynamic evolution vary by 2-3 orders of magnitude (Chiaradia et al., 2014). The genesis of a deposit is effectively instantaneous within the context of a favourable geodynamic setting, being perhaps prompted by a geodynamic trigger (e.g., suturing; magmatism; seismic activity). This effectively instantaneous nature of a mineral deposit is a reflection to some extent of the necessity to concentrate metals, widely distributed in the crust,

into a small space with this focusing in space mirrored also in a focusing in time. Repeated fluid movement along a major structure may transport melts but would more likely to lead to a broad halo of low metal anomalism compared to a brief intense fluid transport event that localizes its metal anomalism. When dealing with the progression of an orogen, we can define a broad time window within which there exist conditions favourable for the formation of a mineral deposit type. Within this framework the actual timescale of deposit formation is considerably shorter.

A time-space plot is presented in Fig. 7. The age constraints from deposits discussed in this paper are presented, along with a postulated time range of potential metallogenesis, which in effect represents the timescale of favourable conditions for the deposit type formation. These are also plotted against the varying hosting lithologies, which are also a proxy for distance from the plate margin.

From this figure we can derive two key observations. Firstly, there exist temporal overlaps of favourable conditions for the formation of a particular deposit type, permitting the genesis of differing metallotects during the same period. For example, we suggest that porphyry-hosted copper and tin-tungsten granite-hosted mineralization have the potential to develop broadly contemporaneously. Secondly, this defines an evolution of the favourable conditions, leading to a genetic sequence of deposit types over the lifetime of an evolving orogen.

More generic application of this template largely depends on the uniqueness of both fertility and favourable crustal architecture. However, both the types of deposit, and the geodynamic settings discussed here for

1109 Myanmar have been commonly documented elsewhere in the world,
1110 especially during the Phanerozoic Eon (e.g., Bierlein et al., 2009).

1111 **8. Conclusions**

1112 We present a metallogenetic model for Myanmar, which
1113 documents the progression of a single orogenic event, and the concomitant
1114 development of a variety of mineralization styles and commodities during its
1115 evolution. We present new age data to underline some of the mineralizatoin
1116 ages within this model. We speculate on the timing of other, poorly age-
1117 constrained deposit types. Our model places the genesis of much of
1118 Myanmar's documented mineral deposits within the context of an evolving
1119 tectonic framework involving the subduction and suturing of the Neo Tethys.
1120

1121 **Acknowledgements**

1122 We are indebted to Andrew Mitchell both for his pioneering work
1123 on, and for introducing us to, the geology and mineral deposits of Myanmar.
1124 NJG acknowledges the Oxford University Fell Fund (Ref. DGD07260) and
1125 Highland Metals Pte Ltd. for financial support. Analytical support at NIGL was
1126 funded through NIGFSC grant IP-1554-0515. U Nyunt Htay is acknowledged
1127 for the sample from Yadanabon Mine. We thank Dave Sansom for drafting
1128 figures; U Kyi Htun for assistance with field logistics; Daw Than Than Nu and
1129 U Ne Lin for accompanying us to Mogok; Thu Htet Aung and Win Zaw for
1130 driving and navigation on various trips; U Htun Lynn Shein for general support
1131 of our Myanmar work. The NordSIM facility is operated under an
1132 agreement between the research funding agencies of Denmark, Iceland,

Norway and Sweden, the Geological Survey of Finland and the Swedish Museum of Natural History, and we thank Kerstin Lindén and Lev Ilyinsky for NordSIM technical support. We are indebted to Tony Barber and Michael Crow for insightful reviews, plus an anonymous reviewer on an earlier version of this manuscript, all of which have greatly improved this work. We thank Franco Pirajno for editorial handling.

References

Acharyya, S.K., 2010. Tectonic evolution of Indo-Burma range with special reference of Naga-Manipur Hills. Geol. Soc. India Mem. 75, 25–43.

Acharyya, S.K., 2007. Collisional emplacement history of the Naga-Andaman ophiolites and the position of the eastern Indian suture. J. Asian Earth Sci. 29, 229–242. doi:10.1016/j.jseaes.2006.03.003

Arribas, A., Hedenquist, J.W., Itaya, T., Okada, T., Concepcion, R. a., Garcia, J.S., 1995. Contemporaneous formation of adjacent porphyry and epithermal Cu-Au deposits over 300 ka in northern Luzon, Philippines. Geology 23, 337–340. doi:10.1130/0091-7613(1995)023<0337:CFOAPA>2.3.CO;2

Aung Zaw Myint, U., Khin Zaw, U., Myint Ye Swe, U., Yonezu, K., Cai, Y., Manaka, T., Watanabe, K., 2016. Geochemistry and geochronology of granites hosting the Mawchi Sn-W deposit, Myanmar: Implications for tectonic setting and granite emplacement, in: Barber, A.J., Crow, M.J., Khin Zaw, U., Rangin, C. (Eds.), Myanmar: Geology, Resources and Tectonics. The Geological Society, London.

Aye Ko Aung, U., 2012. The Palaeozoic stratigraphy of Shan Plateau, Myanmar - an up-dated version. J. Myanmar Geosci. Soc. 5, 1–73.

Barber, A.J., Crow, M.J., 2009. Structure of Sumatra and its implications for the tectonic assembly of Southeast Asia and the destruction of Paleotethys. Isl. Arc 18, 3–20.

Barber, A.J., Crow, M.J., Khin Zaw, U., Rangin, C., 2016. Myanmar: Geology, Resources and Tectonics. The Geological Society, London.

Barley, M.E., Groves, D.I., 1992. Supercontinent cycles and the distribution of metal deposits through time. Geology 20, 291–294. doi:10.1130/0091-7613

Barley, M.E., Khin Zaw, U., 2009. SHRIMP U-Pb in zircon geochronology of granitoids from Myanmar : temporal constraints on the tectonic evolution of Southeast Asia 11, 3842.

1170 Barley, M.E., Pickard, A.L., Khin Zaw, U., Rak, P., Doyle, M.G., 2003.
1171 Jurassic to Miocene magmatism and metamorphism in the Mogok
1172 metamorphic belt and the India-Eurasia collision in Myanmar. Tectonics
1173 22, 1–11. doi:10.1029/2002TC001398

1174 Barr, S.M., Macdonald, A.S., 1991. Toward a late Paleozoic-early Mesozoic
1175 tectonic model for Thailand. Thail. J. Geosci. 1, 11–22.

1176 Begg, G.C., Hronsky, J. a M., Arndt, N.T., Griffin, W.L., O'Reilly, S.Y.,
1177 Hayward, N., 2010. Lithospheric, cratonic, and geodynamic setting of Ni-
1178 Cu-PGE sulfide deposits. Econ. Geol. 105, 1057–1070.
1179 doi:10.2113/econgeo.105.6.1057

1180 Bender, F., 1983. Geology of Burma. Gebriider Borntraeger, Stuttgart.

1181 Bierlein, F.P., Crowe, D.E., 2000. Phanerozoic orogenic lode gold deposits,
1182 in: Reviews in Economic Geology v. 13. Society of Economic Geology,
1183 pp. 103–140.

1184 Bierlein, F.P., Groves, D.I., Cawood, P.A., 2009. Metallogeny of accretionary
1185 orogens - The connection between lithospheric processes and metal
1186 endowment. Ore Geol. Rev. 36, 282–292.
1187 doi:10.1016/j.oregeorev.2009.04.002

1188 Brunnschweiler, R.O., 1966. On the geology of the Indoburman ranges. J.
1189 Geol. Soc. Aust. 13, 137–194.

1190 Burchfiel, B.C., Chen Zhiliang, C., 2013. Tectonics of the Southeastern
1191 Tibetan Plateau and Its Adjacent Foreland. Geol. Soc. Am. Mem. 210, 1–
1192 164. doi:10.1130/2012.1210(01)

1193 Cao, H.-W., Zhang, S.-T., Lin, J.-Z., Zheng, L., Wu, J.-D., Li, D., 2014.
1194 Geology, geochemistry and geochronology of the Jiaojiguanliangzi Fe-
1195 polymetallic deposit, Tengchong County, Western Yunnan (China):
1196 Regional tectonic implications. J. Asian Earth Sci. 81, 142–152.
1197 doi:10.1016/j.jseaes.2013.11.002

1198 Carlson, C. a., 1991. Spatial distribution of ore deposits. Geology 19, 111.
1199 doi:10.1130/0091-7613(1991)019<0111:SDOOD>2.3.CO;2

1200 Cawood, P.A., Hawkesworth, C.J., 2013. Temporal relations between mineral
1201 deposits and global tectonic cycles. Geol. Soc. London, Spec. Publ. 393.
1202 doi:10.1144/sp393.1

1203 Cawood, P.A., Johnson, M.R.W., Nemchin, A.A., 2007. Early Palaeozoic
1204 orogenesis along the Indian margin of Gondwana: Tectonic response to
1205 Gondwana assembly. Earth Planet. Sci. Lett. 255, 70–84.
1206 doi:10.1016/j.epsl.2006.12.006

1207 Charusiri, P., Clark, A.H., Farrar, E., Archibald, D., Charusiri, B., 1993.
1208 Granite belts in Thailand: evidence from the 40Ar/39Ar geochronological
1209 and geological synthesis. J. Southeast Asian Earth Sci. 8, 127–136.

1210 Chen, G.R., Liu, H.F., Jiang, G.W., Zheng, Q.G., Zhao, S.R., Zhang, X.G.,
1211 2004. Discovery of the Shamuluo Formation in the central segment of the
1212 Bangong-Cuo-Nujiang suture zone, Tibet. Geol. Bull. China 23, 193–194.

1213 Chhibber, H.L., 1934. The mineral resources of Burma. Macmillan and Co.,
1214 London.

1215 Chiaradia, M., Schaltegger, U., Spikings, R., 2014. Time Scales of Mineral
1216 Systems — Advances in Understanding Over the Past Decade. Soc.
1217 Econ. Geol. Spec. Publ. 18, 37–58.

1218 Cobbing, E.J., Mallick, D.I.J., Pitfield, P.E.J., Teoh, L.H., 1986. The granites of
1219 the Southeast Asian Tin Belt. J. Geol. Soc. London. 143, 537–550.
1220 doi:10.1144/gsjgs.143.3.0537

1221 Cobbing, E.J., Pitfield, P.E.J., Darbyshire, D., Mallick, D.I.J., Pitfield, P.E.J.,
1222 Teoh, L.H., 1992. The granites of the Southeast Asian Tin Belt. J. Geol.
1223 Soc. London. 143, 537–550. doi:10.1144/gsjgs.143.3.0537

1224 Coggin Brown, J., 1936. India's mineral wealth: A guide to the occurrences
1225 and economics of the useful minerals of the Indian Empire. Oxford
1226 University Press.

1227 Coggin Brown, J., 1918. The cassiterite deposits of Tavoy. Rec. Geol. Surv.
1228 India 49, 23–33.

1229 Coggin Brown, J., Heron, A., 1923. The Geology and Ore Deposits of the
1230 Tavoy District. Mem. Geol. Surv. India 44, 167–354.

1231 Cooper, M.A., Herbert, R., Hill, G.S., 1989. The structural evolution of Triassic
1232 intermontane basins in northeastern Thailand, in: International
1233 Symposium on Intermontane Basins: Geology and Resources. Chiang
1234 Mai, Thailand, Thailand, pp. 231–242.

1235 Cox, R., Gaskell, J., Thomas, C., 1981. Burma: A country with major
1236 unexplored mineral potential, in: Asian Mining '81. Institution of Mining
1237 and Metallurgy, London, pp. 34–45.

1238 Curray, J.R., 2005. Tectonics and history of the Andaman Sea region. J.
1239 Asian Earth Sci. 25, 187–232. doi:10.1016/j.jseaes.2004.09.001

1240 Curray, J.R., Moore, D.G., Lawver, L.A., Emmel, F.J., Raitt, R.W., Henry, M.,
1241 Kieckhefer, R., 1979. Tectonics of the Andaman Sea and Burma, in:
1242 Watkins, T.S., Martadet, L., Dickerson, P.W. (Eds.), Geological and
1243 Geophysical Investigations of Continental Margins. AAPG Memoir, pp.
1244 189–198.

1245 Eskine, T., Khin Zaw, U., Large, R., Makoundi, C., Knight, J., 2015. Geology
1246 and Mineralization Characteristics of the Modi Taung Orogenic Gold
1247 Deposit, Central Myanmar, in: Society of Economic Geologists Annual
1248 Meeting. Hobart, Australia.

1249 Fan, J.-J., Li, C., Xie, C.-M., Wang, M., Chen, J.-W., 2015. Petrology and U–
1250 Pb zircon geochronology of bimodal volcanic rocks from the Maierze
1251 Group, northern Tibet: Constraints on the timing of closure of the
1252 Banggong–Nujiang Ocean. Lithos 227, 148–160.
1253 doi:10.1016/j.lithos.2015.03.021

1254 Franz, L., Tay Thye Sun, U., Hänni, H.A., DeCapitani, C., Thanasuthipitak, T.,
1255 Atichat, W., Sun, T.T., Hänni, H.A., Capitani, C. De, 2014. A Comparative
1256 Study of Jadeite , Omphacite and Kosmochlor Jades from Myanmar , and
1257 Suggestions for a Practical Nomenclature. J. Gemol. 2, 210–229.

1258 Fraser, G.L., Huston, D.L., Gibson, G.M., Neumann, N.L., Maidment, D.,
1259 Kositcin, N., Skirrow, R.G., Jaireth, S., Lyons, P., Carson, C., Cutten, H.,

Lambeck, A., 2007. Geodynamic and Metallogenic Evolution of Proterozoic Australia from 1870 - 1550 Ma: a discussion (No. 2007/16), Geoscience Australia Record.

Gardiner, N.J., Robb, L.J., Searle, M.P., 2014. The metallogenic provinces of Myanmar. Appl. Earth Sci. 123, 25–38. doi:10.1179/1743275814Y.0000000049

Gardiner, N.J., Robb, L.J., Searle, M.P., Kyi Htun, U., Khin Zaw, U., 2016. The Bawdwin Mine: A Review of its Geological Setting and Genesis, in: Barber, A.J., Crow, M.J., Khin Zaw, U., Rangin, C. (Eds.), Myanmar: Geology, Resources and Tectonics. The Geological Society, London.

Gardiner, N.J., Searle, M.P., Morley, C.K., Whitehouse, M.P., Spencer, C.J., Robb, L.J., 2015a. The closure of Palaeo-Tethys in Eastern Myanmar and Northern Thailand: New insights from zircon U–Pb and Hf isotope data. Gondwana Res. doi:10.1016/j.gr.2015.03.001

Gardiner, N.J., Searle, M.P., Robb, L.J., Morley, C.K., 2015b. Neo-Tethyan Magmatism and Metallogeny in Myanmar – an Andean Analogue? J. Asian Earth Sci. doi:10.1016/j.jseaes.2015.03.015

Garnier, V., Giuliani, G., Ohnenstetter, D., Fallick, A.E., Dubessy, J., Banks, D., Vinh, H.Q., Lhomme, T., Maluski, H., Pêcher, A., Bakhsh, K.A., Long, P. Van, Trinh, P.T., Schwarz, D., 2008. Marble-hosted ruby deposits from Central and Southeast Asia: Towards a new genetic model. Ore Geol. Rev. 34, 169–191. doi:10.1016/j.oregeorev.2008.03.003

Garnier, V., Maluski, H., Giuliani, G., Ohnenstetter, D., Schwarz, D., 2006. Ar–

-Ar and U–-Pb ages of marble-hosted ruby deposits from central and southeast Asia. Can. J. Earth Sci. 43, 509–532. doi:10.1139/e06-005

Garson, M.S., Amos, B.J., Mitchell, A.H.G., 1976. The geology of the area around Neyaungga and Yengan, Southern Shan State, Burma (No. 2:70), Overseas Memoir.

Garzanti, E., Baud, A., Mascle, G., 1987. Sedimentary record of the northward flight of India and its collision with Eurasia (Ladakh Himalaya, India). Geodin. Acta 1, 297–312.

Ghose, N.C., Chatterjee, N., Fareeduddin, 2014. A Petrographic Atlas of Ophiolite, An example from the eastern India-Asia collision zone. Springer India.

Goffe, B., Rangin, C., Maluski, H., 2002. Jade and associated rocks from the jade Mines area, Northern Myanmar as record of a polyphased high pressure metamorphism, in: Himalaya - Karakoram - Tibet Workshop Meeting, Abstract: Journal of Asian Earth Sciences.

Goldfarb, R.J., Baker, T., Dube, D., Groves, D.I., Hart, C.J.R., Gosselin, P., 2005. Distribution, character and genesis of gold deposits in metamorphic terranes, in: Hedenquist, J.W., Thompson, J.F.H., Goldfarb, R.J., Richards, J.P. (Eds.), Economic Geology 100th Anniversary Volume. pp. 407–450.

Goldfarb, R.J., Groves, D.I., 2015. Orogenic gold: Common or evolving fluid and metal sources through time. Lithos 233, 2–26.

1305 doi:10.1016/j.lithos.2015.07.011

1306 Goossens, P., 1979. The metallogenic provinces of Burma: Their definitions,
1307 geologic relationships and extension into China, India and Thailand, in:
1308 Third Regional Conference on Geology and Mineral Resources of
1309 Southeast Asia.

1310 Green, O.R., Searle, M.P., Corfield, R.I., Corfield, R.M., 2008. Cretaceous-
1311 Tertiary Carbonate Platform Evolution and the Age of the India-Asia
1312 Collision along the Ladakh Himalaya (Northwest India). J. Geol. 116,
1313 331–353. doi:10.1086/588831

1314 Griffith, S., 1956. The mineral resources of Burma. Mineral. Mag. 95, 9–18.

1315 Groves, D.I., Bierlein, F.P., 2007. Geodynamic settings of mineral deposit
1316 systems. J. Geol. Soc. London. 164, 19–30. doi:10.1144/0016-76492006-
1317 065

1318 Groves, D.I., Goldfarb, R.J., Gebre-Mariam, M. Hagemann, S.G., Robert, F.,
1319 1998. Orogenic gold deposits: A proposed classification in the context of
1320 their crustal distribution and relationship to other gold deposit types. Ore
1321 Geol. Rev. 13, 7–27.

1322 Hall, R., 2012. Late Jurassic–Cenozoic reconstructions of the Indonesian
1323 region and the Indian Ocean. Tectonophysics 570-571, 1–41.
1324 doi:10.1016/j.tecto.2012.04.021

1325 Hammarstrom, J.M., Bookstrom, A.A., Dicken, C.L., Drenth, B.J., Ludington,
1326 S., Robinson, G.R., Tjahjono Setiabudi, B., Sukserm, W., Nugroho
1327 Sunuhadi, D., Yan Sze Wah, A., Zientek, M.L., 2010. Porphyry Copper
1328 Assessment of Southeast Asia and Melanesia.

1329 Hedenquist, J.W., Lowenstern, J.B., 1994. The role of magmas in the
1330 formation of hydrothermal ore deposits. Nature 370, 519–527.
1331 doi:10.1038/370519a0

1332 Hobson, G.V., 1940. The Development of the mineral deposit at Mawchi as
1333 determined by geology and genesis. Trans. Min. Geol. Metall. Inst. India
1334 36, 35–78.

1335 Hughes, R.W., Galibert, O., Bosshart, G., Ward, F., Thet Oo, U., Smith, M.,
1336 Tay Thye Sun, U., Harlow, G.E., 2000. Burmese Jade: The Inscrutable
1337 Gem. Gems Gemol. 36, 2–26.

1338 Hutchison, C.S., 1994. Gondwana and Cathaysian blocks, palaeotethys
1339 sutures and cenozoic tectonics in South-east Asia. Geol. Rundschau 83,
1340 388–405.

1341 Hutchison, C.S., 1975. Ophiolite in Southeast Asia. Bull. Geol. Soc. Am. 86,
1342 797–806. doi:10.1130/0016-7606(1975)86<797:OISA>2.0.CO;2

1343 Hutchison, C.S., Taylor, D., 1978. Metallogenesis in SE Asia. J. Geol. Soc.
1344 London. 135, 407–428. doi:10.1144/gsjgs.135.4.0407

1345 Iyer, L.A.N., 1953. The geology and gemstones of the Mogok Stone Tract,
1346 Burma. Geol. Soc. India Mem. 82, 100.

1347 Kerrich, R., Goldfarb, R.J., Richards, J.P., 2005. Metallogenic Provinces in an
1348 Evolving Geodynamic Framework, in: Hedenquist, J.W., Thompson,
1349 J.F.H., Goldfarb, R.J., Richards, J.P. (Eds.), Economic Geology 100th

1350 Anniversary Volume. pp. 1097–1136.

1351 Khin Zaw, U., 1990. Geological, petrogical and geochemical characteristics of
1352 granitoid rocks in Burma: with special reference to the associated WSn
1353 mineralization and their tectonic setting. J. Southeast Asian Earth Sci. 4,
1354 293–335.

1355 Khin Zaw, U., Khin Myo Thet, U., 1983. A note on a fluid inclusion study of tin-
1356 tungsten mineralization at Mawchi Mine, Kayah State, Burma. Econ.
1357 Geol. 78, 530–534.

1358 Khin Zaw, U., Meffre, S., Lai, C.K., Burrett, C., Santosh, M., Graham, I.,
1359 Manaka, T., Salam, A., Kamvong, T., Cromie, P., 2014. Tectonics and
1360 metallogeny of mainland Southeast Asia - A review and contribution.
1361 Gondwana Res. 26, 5–30. doi:10.1016/j.gr.2013.10.010

1362 Khin Zaw, U., Pwa Zan, Thet Aung, A., Wung Pwa, U., Thet Aung Zan, U.,
1363 1984. Lead-zinc mineralization at Theingon Mine, Bawsaing, Southern
1364 Shan State, Burma: A Mississippi Valley-type deposit ? Bull. Geol. Soc.
1365 Malaysia 17, 283–306.

1366 Kirkland, C.L., Daly, J.S., Whitehouse, M.J., 2008. Basement-cover
1367 relationships of the Kalak Nappe Complex, Arctic Norwegian Caledonides
1368 and constraints on Neoproterozoic terrane assembly in the North Atlantic
1369 region. Precambrian Res. 160, 245–276.
1370 doi:10.1016/j.precamres.2007.07.006

1371 Leach, D., Sangster, D., Kelley, D., Large, R.R., Garven, G., Allen, C.,
1372 Gutzmer, J., Walters, S.G., 2005. Sediment-hosted lead-zinc deposits: A
1373 global perspective, in: Hedenquist, J.W., Thompson, J.F.H., Goldfarb,
1374 R.J., Richards, J.P. (Eds.), Economic Geology 100th Anniversary
1375 Volume. pp. 561–608.

1376 Lin, Y.-L., Yeh, M.-W., Lee, T.-Y., Chung, S.-L., Iizuka, Y., Charusiri, P., 2013.
1377 First evidence of the Cambrian basement in Upper Peninsula of Thailand
1378 and its implication for crustal and tectonic evolution of the Sibumasu
1379 terrane. Gondwana Res. 24, 1031–1037.

1380 Ludwig, K.R., 2004. User's manual for Isoplot, 3.16: A Geochronological
1381 Toolkit for Microsoft Excel. Berkeley Geochronology Center Special
1382 Publication, Ridge Road, Berkeley CA, USA, Berkeley, USA.

1383 Ludwig, K.R., 1998. On the Treatment of Concordant Uranium-Lead Ages.
1384 Geochim. Cosmochim. Acta 62, 665–676. doi:10.1016/S0016-
1385 7037(98)00059-3

1386 Maurin, C., Masson, F., Rangin, C., Than Min, U., Collard, P., 2010. First
1387 global positioning system results in northern Myanmar: Constant and
1388 localized slip rate along the Sagaing Fault. Geology 38, 591–594.

1389 Maurin, T., Rangin, C., 2009. Structure and kinematics of the Indo-Burmese
1390 wedge: rapid and fast growth of the outer wedge. Tectonics 28, 1–21.

1391 Maury, R.C., Pubellier, M., Rangin, C., Wulput, L., Cotten, J., Socquet, A.,
1392 Bellon, H., Guillaud, J.-P., Hla Myo Htun, U., 2004. Quaternary calc-
1393 alkaline and alkaline volcanism in an hyper-oblique convergence setting,
1394 central Myanmar and western Yunnan. Bull. la Société Géologique Fr.
1395 175, 461–472.

McCuaig, T., Hronsky, J.M.A., 2014. The Mineral System Concept : The Key to Exploration Targeting. Soc. Econ. Geol. Spec. Publ. 18, 153–175.

McCuaig, T.C., Beresford, S., Hronsky, J., 2010. Translating the mineral systems approach into an effective exploration targeting system. Ore Geol. Rev. 38, 128–138. doi:10.1016/j.oregeorev.2010.05.008

Metcalfe, I., 2013. Gondwana dispersion and Asian accretion: Tectonic and palaeogeographic evolution of eastern Tethys. J. Asian Earth Sci. 66, 1–33. doi:10.1016/j.jseaes.2012.12.020

Metcalfe, I., 2011. Palaeozoic-Mesozoic history of SE Asia, in: Hall, R., Cottam, M.A., Wilson, M.E.J. (Eds.), The SE Asian Gateway: History and Tectonics of the Australia-Asia Collision. Geological Society, London Special Publication, pp. 7–35. doi:10.1144/SP355.2

Metcalfe, I., 2006. Palaeozoic and Mesozoic tectonic evolution and palaeogeography of East Asian crustal fragments: The Korean Peninsula in context. Gondwana Res. 9, 24–46. doi:10.1016/j.gr.2005.04.002

Metcalfe, I., 2002. Permian tectonic framework and palaeogeography of SE Asia. J. Asian Earth Sci. 20, 551–566. doi:10.1016/S1367-9120(02)00022-6

Metcalfe, I., 2000. The Bentong – Raub Suture Zone. J. Asian Earth Sci. 18, 691–712.

Metcalfe, I., 1984. Stratigraphy, palaeontology and palaeogeography of the Carboniferous of Southeast Asia. Mémoires la Société Géographique Fr. 147, 107–118.

MGS, 2012. Geological Map of Myanmar. Myanmar Geosciences Society, Yangon.

Mitchell, A.H.G., 1993. Cretaceous-Cenozoic tectonic events in the western Myanmar (Burma)-Assam region. J. Geol. Soc. London. 150, 1089–1102. doi:10.1144/gsjgs.150.6.1089

Mitchell, A.H.G., 1992. Late Permian-Mesozoic events and the Mergui Group nappe in Myanmar and Thailand. J. Southeast Asian Earth Sci. 7, 165–178.

Mitchell, A.H.G., 1986. Mesozoic and Cenozoic regional tectonics and metallogenesis in Mainland SE Asia. Geo. Soc. Malaysia Bull. 20, 221–239.

Mitchell, A.H.G., 1979. Rift-, Subduction- and Collision-Related Tin Belts. Geol. Soc. Malaysia Bull. 11, 81–102.

Mitchell, A.H.G., 1977. Tectonic settings for the emplacement of Southeast Asian tin granites. Geol. Soc. Malaysia Bull. 9, 123–140.

Mitchell, A.H.G., Ausa, C.A., Deiparine, L., Hlaing, T., Htay, N., Khine, A., 2004. The Modi Taung - Nankwe gold district, Slate belt, central Myanmar: Mesothermal veins in a Mesozoic orogen. J. Asian Earth Sci. 23, 321–341. doi:10.1016/S1367-9120(03)00138-X

Mitchell, A.H.G., Chung, S.-L., Oo, T., Lin, T.H., Hung, C.H., 2012. Zircon U-Pb ages in Myanmar: Magmatic-metamorphic events and the closure of a neo-Tethys ocean? J. Asian Earth Sci. 56, 1–23.

1441 doi:10.1016/j.jseaes.2012.04.019

1442 Mitchell, A.H.G., Garson, M.S., 1981. Mineral Deposits and Global Tectonic
1443 Settings. Academic Press, New York.

1444 Mitchell, A.H.G., Htay, M.T., 2013. The Magmatic Arc and the Slate Belt:
1445 Copper-gold and Tin-tungsten and Gold Metallotects in Myanmar. East
1446 Asia: Geology, Exploration Techniques and Mines, Bali, pp. 58–59.

1447 Mitchell, A.H.G., McKerrow, W.S., 1975. Analogous Evolution of the Burma
1448 Orogen and the Scottish Caledonides. Bull. Geol. Soc. Am. 86, 305–315.
1449 doi:10.1130/0016-7606(1975)86<305:AEOTBO>2.0.CO;2

1450 Mitchell, A.H.G., Myint Thein Htay, U., Kyaw Min Htun, U., 2015. The Medial
1451 Myanmar Suture Zone and the Western Myanmar- Mogok foreland. J.
1452 Myanmar Geosci. Soc. 6, 73–88.

1453 Mitchell, A.H.G., Myint Thein Htay, U., Kyaw Min Htun, U., Myint Naing Win,
1454 U., Thura Oo, U., Tin Hlaing, U., 2007. Rock relationships in the Mogok
1455 metamorphic belt, Tatkon to Mandalay, central Myanmar. J. Asian Earth
1456 Sci. 29, 891–910. doi:10.1016/j.jseaes.2006.05.009

1457 Mitchell, A.H.G., Nyunt Htay, U., Ausa, C., Deiparine, L., Aung Khine, U., Sein
1458 Po, U., 1999. Geological Settings of Gold Districts in Myanmar. Semin.
1459 Pacrim Berli.

1460 Mitchell, A.H.G., Win Myint, U., Kyi Lynn, U., Myint Thein Htay, U., Maw Oo,
1461 U., Thein Zaw, U., 2011. Geology of the High Sulfidation Copper
1462 Deposits, Monywa Mine, Myanmar. Resour. Geol. 61, 1–29.
1463 doi:10.1111/j.1751-3928.2010.00145.x

1464 Mitra, S., Priestley, K., Bhattacharyya, A.K., Gaur, V.K., 2005. Crustal
1465 structure and earthquake focal depths beneath northeastern India and
1466 southern Tibet. Geophys. J. Int. 160, 227–248.

1467 Morley, C.K., 2012. Late Cretaceous-Early Palaeogene tectonic development
1468 of SE Asia. Earth-Science Rev. 115, 37–75.
1469 doi:10.1016/j.earscirev.2012.08.002

1470 Myint, K.K., 1994. Mineral Belts and Epochs in Myanmar. Resour. Geol. 44,
1471 1–3.

1472 Ng, S.W.P., Chung, S.-L., Robb, L.J., Searle, M.P., Ghani, A.A., Whitehouse,
1473 M.J., Oliver, G.J.H., Sone, M., Gardiner, N.J., Roselee, M.H., 2015.
1474 Petrogenesis of Malaysian granitoids in the Southeast Asian tin belt: Part
1475 1. Geochemical and Sr-Nd isotopic characteristics. Geol. Soc. Am. Bull.
1476 1–29. doi:10.1130/B31213.1

1477 Nielsen, C., Chamot-Rooke, N., Rangin, C., 2004. From partial to full strain
1478 partitioning along the Indo-Burmese hyper-oblique subduction. Mar. Geol.
1479 209, 303–327. doi:10.1016/j.margeo.2004.05.001

1480 Otofuji, Y., Mu, C.L., Tanaka, K., Miura, D., Inokuchi, H., Kamei, R., Tamai,
1481 M., Takemoto, K., Zaman, H., Yokoyama, M., 2007. Spatial gap between
1482 Lhasa and Qiangtang blocks inferred from Middle Jurassic to Cretaceous
1483 paleomagnetic data. Earth Planet. Sci. Lett. 262, 581–593.
1484 doi:10.1016/j.epsl.2007.08.013

1485 Pollard, P., Nakapadungrat, S., Taylor, R., 1995. The Phuket Supersuite,

1486 Southwest Thailand: Fractionated I-Type Granites Associated with Tin-
1487 Tantalum Mineralization. Econ. Geol. 90, 586–602.

1488 Rangin, C., Maurin, T., Masson, F., 2013. Combined effects of Eurasia/Sunda
1489 oblique convergence and East-Tibetan crustal flow on the active tectonics
1490 of Burma. J. Asian Earth Sci. 76, 185–194.
1491 doi:10.1016/j.jseaes.2013.05.018

1492 Raterman, N.S.S., Robinson, A.C.C., Cowgill, E.S.S., 2014. Structure and
1493 detrital zircon geochronology of the Domar fold-thrust belt: Evidence of
1494 pre-Cenozoic crustal thickening of the western Tibetan Plateau. Geol.
1495 Soc. Am. Spec. Pap. 507 , 89–104. doi:10.1130/2014.2507(05)

1496 Replumaz, A., Tapponnier, P., 2003. Reconstruction of the deformed collision
1497 zone Between India and Asia by backward motion of lithospheric blocks.
1498 J. Geophys. Res. 108, 2285. doi:10.1029/2001JB000661

1499 Reynolds, N. a., Chisnall, T.W., Kaewsang, K., Keesaneyabutr, C.,
1500 Taksavasu, T., 2003. The Padaeng supergene nonsulfide zinc deposit,
1501 Mae Sod, Thailand. Econ. Geol. 98, 773–785.
1502 doi:10.2113/gsecongeo.98.4.773

1503 Richards, J.P., 2014. Tectonic, magmatic, and metallogenic evolution of the
1504 Tethyan orogen: From subduction to collision. Ore Geol. Rev. 70, 323–
1505 345. doi:10.1016/j.oregeorev.2014.11.009

1506 Ridd, M.F., 2016. Karen-Tenasserim Unit, in: Barber, A.J., Crow, M.J., Khin
1507 Zaw, U., Rangin, C. (Eds.), Myanmar: Geology, Resources and
1508 Tectonics. Geological Society, London.

1509 Ridd, M.F., 2015. Should Sibumasu be renamed Sibuma? The case for a
1510 discrete Gondwana-derived block embracing western Myanmar, upper
1511 Peninsular Thailand and NE Sumatra. J. Geol. Soc. London. 2015–065.
1512 doi:10.1144/jgs2015-065

1513 Ridd, M.F., 2009. The Phuket Terrane: A Late Palaeozoic rift at the margin of
1514 Sibumasu. J. Asian Earth Sci. 36, 238–251.
1515 doi:10.1016/j.jseaes.2009.06.006

1516 Ridd, M.F., Watkinson, I., 2013. Phuket-Slate Belt terrane: tectonic evolution
1517 and strike-slip emplacement of a major terrane on the Sundaland margin
1518 of Thailand and Myanmar. Proc. Geol. Assoc. 124, 994–1010.

1519 Robb, L.J., 2004. Introduction to Ore-Forming Processes. Blackwell, Oxford.

1520 Sanematsu, K., Manaka, T., Khin Zaw, U., 2014. Geochemical and
1521 Geochronological Characteristics of Granites and Sn-W-REE
1522 Mineralization in the Thanintharyi Region, Southern Myanmar. GEOSEA
1523 XIII Proc. 19–20.

1524 Schellmann, W., 1989. Composition and origin of lateritic nickel ore at
1525 Tagaung Taung, Burma. Miner. Depos. 24, 161–168.
1526 doi:10.1007/BF00206438

1527 Searle, D.L., Ba Than Haq, U., 1964. The Mogok belt of Burma and its
1528 relationship to the Himalayan orogeny, in: Proceedings of the 22nd
1529 International Geological Conference. Delhi, pp. 132–161.

1530 Searle, M.P., Cooper, D.J., Rex, A.J., 1988. Collision tectonics of the Ladakh-

Zanskar Himalaya. Philos. Trans. R. Soc. London 326, 117–150.

Searle, M.P., Morley, C.K., 2011. Tectonics and thermal evolution of Thailand in the regional context of Southeast Asia, in: Ridd, M.F., Barber, A.J., Crow, M.J. (Eds.), The Geology of Thailand. The Geological Society, London, pp. 539–572.

Searle, M.P., Morley, C.K., Waters, D.J., Gardiner, N.J., Kyi Htun, U., Robb, L.J., 2016. Tectonics of the Mogok Metamorphic Belt, Myanmar (Burma) and its correlations from the East Himalayan Syntaxis to the Malay Peninsula, in: Barber, A.J., Crow, M.J., Khin Zaw, U., Rangin, C. (Eds.), Myanmar: Geology, Resources and Tectonics. The Geological Society, London.

Searle, M.P., Noble, S.R., Cottle, J.M., Waters, D.J., Mitchell, A.H.G., Tin Hlaing, U., Horstwood, M.S.A., 2007. Tectonic evolution of the Mogok metamorphic belt, Burma (Myanmar) constrained by U-Th-Pb dating of metamorphic and magmatic rocks. Tectonics 26. doi:10.1029/2006TC002083

Sevastjanova, I., Hall, R., Rittner, M., Saw Mu Tha Lay Paw, U., Tin Tin Naing, D., Alderton, D.H., Comfort, G., 2015. Myanmar and Asia united, Australia left behind long ago. Gondwana Res. doi:10.1016/j.gr.2015.02.001

Sillitoe, R.H., 1972. Relation of Metal Provinces in Western America to Subduction of Oceanic Lithosphere. Geol. Soc. Am. Bull. 83, 813–818. doi:10.1130/0016-7606(1972)83

Socquet, A., Vigny, C., Chamot-Rooke, N., Simons, W., Rangin, C., Ambrosius, B., 2006. India and Sunda plates motion and deformation along their boundary in Myanmar determined by GPS. J. Geophys. Res. Solid Earth 111, 1–11. doi:10.1029/2005JB003877

Soe Win, U., Malar Myo Myint, U., 1998. Mineral Potential of Myanmar. Resour. Geol. 48, 209–218.

Sone, M., Metcalfe, I., 2008. Parallel Tethyan sutures in mainland Southeast Asia: New insights for Palaeo-Tethys closure and implications for the Indosinian orogeny. Comptes Rendus - Geosci. 340, 166–179. doi:10.1016/j.crte.2007.09.008

Spencer, C.J., Roberts, N.M.W., Cawood, P.A., Hawkesworth, C.J., Prave, A.R., Antonini, A.S.M., Horstwood, M.S.A., 2014. Intermontane basins and bimodal volcanism at the onset of the Sveconorwegian Orogeny, southern Norway. Precambrian Res. 252, 107–118. doi:10.1016/j.precamres.2014.07.008

Stacey, J.S., Kramers, J.D., 1975. Approximation of terrestrial lead isotope evolution by a two-stage model. Earth Planet. Sci. Lett. 26, 207–221. doi:10.1016/0012-821X(75)90088-6

Stephenson, D., Marshall, T.R., 1984. The petrology and mineralogy of Mt. Popa Volcano and the nature of the late-Cenozoic Burma Volcanic Arc. J. Geol. Soc. London. 141, 747–762. doi:10.1144/gsjgs.141.4.0747

Stern, R.J., Scholl, D.W., 2010. Yin and yang of continental crust creation and destruction by plate tectonic processes. Int. Geol. Rev. 52, 1–31.

1577 doi:10.1080/00206810903332322

1578 Stork, A.L., Selby, N.D., Heyburn, R., Searle, M.P., 2008. Accurate Relative
1579 Earthquake Hypocenters Reveal Structure of the Burma Subduction
1580 Zone. Bull. Seismol. Soc. Am. 98, 2815–2827.

1581 Suzuki, H., Maung Maung, U., Aye Ko Aung, U., Takai, M., 2004. Jurassic
1582 radiolarian from chert pebbles of the Eocene Pondaung Formation,
1583 central Myanmar. Neues Jahrb. fur Geol. und Palaontologie 231, 369–
1584 393.

1585 Themelis, T., 2008. Gems & Mines Of Mogok. A&T Pub. (USA).

1586 Tin Aung Myint, U., Than Than Nu, D., Min Aung, U., 2014. Precious and
1587 Base Metal Mineralization in Kwinthonze-Nweyon area, Singu and
1588 Thabeikkyin Townships, Mandalay Region, Myanmar, in: Sundaland
1589 Resources. Indonesia.

1590 UNDP, 1996. Geology and mineral resources of Myanmar. Atlas of the
1591 Mineral Regions of the ESCAP Region (No. 12), United Nations
1592 Economic and Social Commission for Asia and the Pacific.

1593 UNDP, 1978. Geology and exploration geochemistry of the Pinlebu-Banmauk
1594 area, Sagaing Division, Northern Burma, Geological Survey and
1595 Exploration Project. New York.

1596 Vigny, C., 2003. Present-day crustal deformation around Sagaing fault,
1597 Myanmar. J. Geophys. Res. 108. doi:10.1029/2002JB001999

1598 Wang, B.-D., Wang, L.-Q., Chung, S.-L., Chen, J.-L., Yin, F.-G., Liu, H., Li, X.-
1599 B., Chen, L.-K., 2015. Evolution of the Bangong–Nujiang Tethyan ocean:
1600 Insights from the geochronology and geochemistry of mafic rocks within
1601 ophiolites. Lithos. doi:10.1016/j.lithos.2015.07.016

1602 Wang, J.G., Wu, F.Y., Tan, X.C., Liu, C.Z., 2014. Magmatic evolution of the
1603 Western Myanmar Arc documented by U-Pb and Hf isotopes in detrital
1604 zircon. Tectonophysics 612-613, 97–105. doi:10.1016/j.tecto.2013.11.039

1605 Wang, Y., Xing, X., Cawood, P.A., Lai, S., Xia, X., Fan, W., Liu, H., Zhang, F.,
1606 2013. Petrogenesis of early Paleozoic peraluminous granite in the
1607 Sibumasu Block of SW Yunnan and diachronous accretionary orogenesis
1608 along the northern margin of Gondwana. Lithos 182-183, 67–85.
1609 doi:10.1016/j.lithos.2013.09.010

1610 Whitehouse, M.J., Kamber, B.S., 2005. Assigning dates to thin gneissic veins
1611 in high-grade metamorphic terranes: A cautionary tale from Akilia,
1612 southwest Greenland. J. Petrol. 46, 291–318.
1613 doi:10.1093/petrology/egh075

1614 Whitehouse, M.J., Kamber, B.S., Moorbath, S., 1999. Age significance of U–
1615 Th–Pb zircon data from early Archaean rocks of west Greenland—a
1616 reassessment based on combined ion-microprobe and imaging studies.
1617 Chem. Geol. 160, 201–224. doi:10.1016/S0009-2541(99)00066-2

1618 Ye Myint Swe, U., Lee, I.S., Than Htay, U., Min Aung, U., 2004. Gold
1619 mineralization at the Kyaukpahto mine area, northern Myanmar. Resour.
1620 Geol. 54, 197–204.

1621 Yui, T.-F., Fukoyama, M., Iizuka, Y., Wu, C.-M., Wu, T.-W., Liou, J.G., Grove,

M., 2013. Is Myanmar jadeitite of Jurassic age? A result from incompletely recrystallized inherited zircon. Lithos 160-161, 268–282. doi:10.1016/j.lithos.2012.12.011

Zahirovic, S., Seton, M., Müller, R.D., 2014. The Cretaceous and Cenozoic tectonic evolution of Southeast Asia. Solid Earth 5, 227–273. doi:10.5194/se-5-227-2014

Zaw Naing Oo, U., Khin Zaw, U., 2009. Geology and mineralization characteristics of Meyon gold deposit, Mon State, Southern Myanmar, in: Proceedings of the Eleventh Regional Congress on Geology, Mineral and Energy Resources of Southeast Asia (GEOSEA). Kuala Lumpur, Malaysia, p. 32.

Zhao, S., Lai, S., Qin, J., Zhu, R.-Z., 2015. Tectono-magmatic evolution of the Gaoligong belt, southeastern margin of the Tibetan plateau: Constraints from granitic gneisses and granitoid intrusions. Gondwana Res. doi:10.1016/j.gr.2015.05.007

Zhu, D.-C., Li, S.-M., Cawood, P.A.A., Wang, Q., Zhao, Z.-D., Liu, S.-A., Wang, L.-Q., 2015. Assembly of the Lhasa and Qiangtang terranes in central Tibet by divergent double subduction. Lithos. doi:10.1016/j.lithos.2015.06.023

Zhu, D.-C., Zhao, Z.-D., Niu, Y., Dilek, Y., Wang, Q., Ji, W.-H., Dong, G.-C., Sui, Q.-L., Liu, Y.-S., Yuan, H.-L., Mo, X.-X., 2012. Cambrian bimodal volcanism in the Lhasa Terrane, southern Tibet: Record of an early Paleozoic Andean-type magmatic arc in the Australian proto-Tethyan margin. Chem. Geol. 328, 290–308. doi:10.1016/j.chemgeo.2011.12.024

Zi, J.W., Cawood, P.A., Fan, W.M., Wang, Y.J., Tohver, E., McCuaig, T.C., Peng, T.P., 2012. Triassic collision in the Paleo-Tethys Ocean constrained by volcanic activity in SW China. Lithos 144-145, 145–160. doi:10.1016/j.lithos.2012.04.020

Fig. 1. Geological terrane map of the Eastern Himalaya, southeast Tibet, Myanmar, Yunnan (China), and Thailand. ITPS – Indus-Tsangpo suture zone; SH – Shillong plateau; SFZ – Sagaing fault zone; TPFZ – Three Pagodas Fault zone; MPFZ – Mae Ping Fault zone; PFZ - Paung Laung Fault Zone; ST – Sibumasu; ASRR – Ailao Shan – Red River shear zone; SCT – South China terrane; EHS = Eastern Himalayan Syntaxis. WB = Western Ophiolite Belt; EB = Eastern Ophiolite Belt. From Gardiner et al. (2015b).

Fig. 2. Palaeogeographic reconstructions for the Eastern Tethys during the Late Jurassic, Early Cretaceous, Late Cretaceous and Middle Eocene. Simplified from Metcalfe (2011). S = Sibumasu; I = Indochina; SC = South China; QS = Qamdo-Simao. The Mawgyi Arc and the putative West Burma Plate (WB) are highlighted.

Fig. 3. Geological map of Myanmar, detailing the main geological provinces, and the major deposits as discussed in the text. Based on the Myanmar Geosciences Geological Map of Myanmar (MGS, 2012).

Fig. 4. Concordia diagrams showing ^{20} Pb-corrected zircon U-Pb ages, and ^{207}Pb-corrected age weighted average plots, for all samples selected for calculation of Concordia ages. All uncertainty bars are 2 sigma.

Fig. 5. Diagrams showing the interpreted metallogenetic settings for a number of ore deposit types discussed in the text. (a) Schematic continental crust architecture during the accretionary stage with relevant magmatic-related ore deposits; (b) Hypothetical Slate Belt Orogenic Au mineralization; prograde metamorphism of Mogok rocks at depth releases fluids that migrate into lower-grade brittle upper crust; (c) A model for the Kyaukpahto epithermal gold mine: en-echelon strike-slip fault arrays associated with extensional stresses related to movement on the Sagaing Fault. Diagrams a and c modified from Robb (2004). Diagram b modified after Groves et al. (1998) and Goldfarb and Groves (2015).

Fig. 6. Schematic tectonic evolution of Myanmar, detailing interpreted metallogenesis related to each major stage and location of major mines.

Fig. 7. Space-time chart constructed for Myanmar, showing ages of major deposits discussed in the text.

Table 1: Summary of samples, localities and age data. All age uncertainties are quoted at 2 sigma. MMM = Mogok-Mandalay-Mergui Belt; WPA = Wuntho-Popa Arc.

Table 2: Full U-Pb analyses. Errors quoted are 1σ. ^{207}Pb-corrected ages calculated as per (Ludwig, 1998).
$^{\dagger}f_{206}$%: % of common ^{206}Pb estimated from measured ^{204}Pb. Figures in parentheses are given when no common Pb correction is made (because of low ^{204}Pb levels), indicating a value calculated assuming present-day Stacey-Kramers common Pb.

Table 3: Metallotects of Myanmar discussed in the text.

Figure 1:

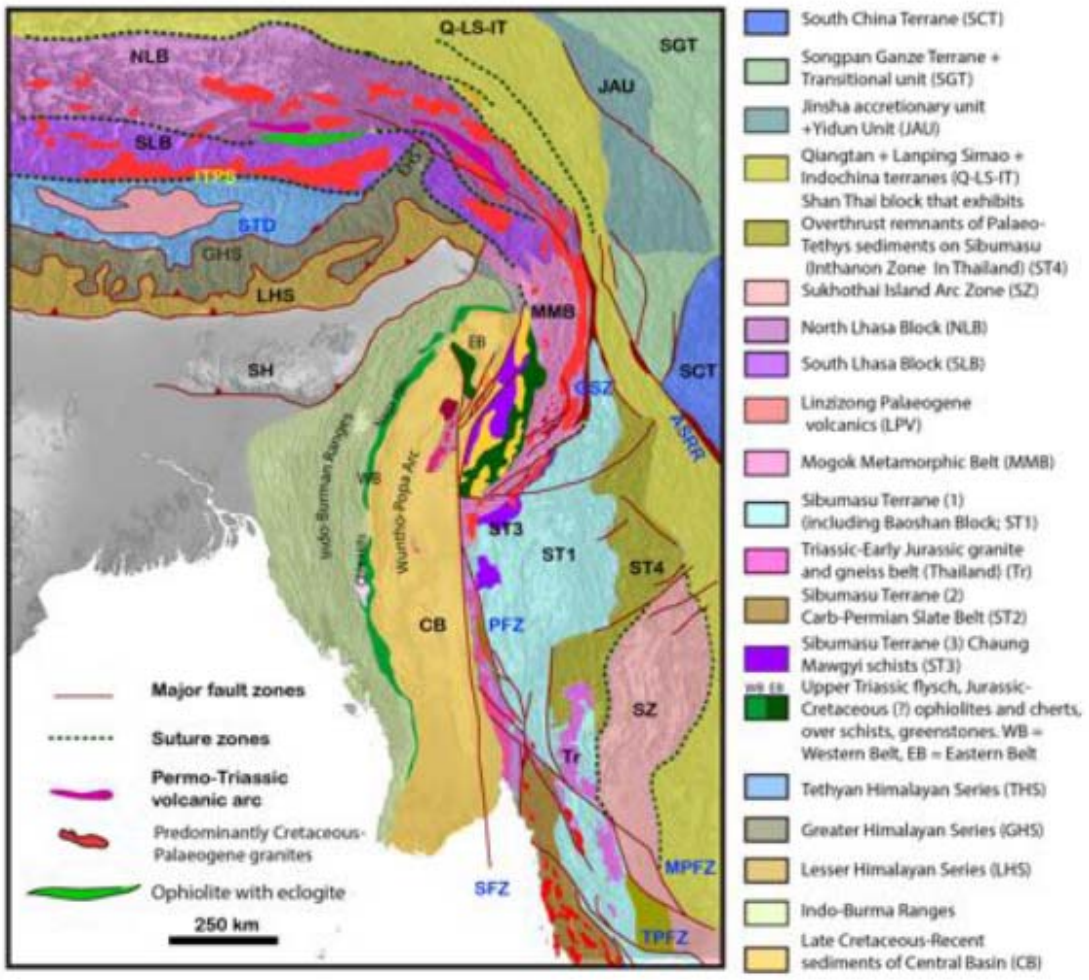
Q-LS-IT
NLB
SLB
ITSZ
STD
GHS
LHS
SH
SGT
JAU
MMB
EB
SCT
GSZ
ASRR
Indo-Burman Ranges
Wuntho-Popa Arc
ST3
ST1
ST4
CB
PFZ
SZ
Tr
MPFZ
SFZ
TPFZ
Major fault zones
Suture zones
Permo-Triassic volcanic arc
Predominantly Cretaceous-Palaeogene granites
Ophiolite with eclogite
250 km
South China Terrane (SCT)
Songpan Ganze Terrane + Transitional unit (SGT)
Jinsha accretionary unit +Yidun Unit (JAU)
Qiangtan + Lanping Simao + Indochina terranes (Q-LS-IT)
Shan Thai block that exhibits Overthrust remnants of Palaeo-Tethys sediments on Sibumasu (Inthanon Zone In Thailand) (ST4)
Sukhothai Island Arc Zone (SZ)
North Lhasa Block (NLB)
South Lhasa Block (SLB)
Linzizong Palaeogene volcanics (LPV)
Mogok Metamorphic Belt (MMB)
Sibumasu Terrane (1) (including Baoshan Block; ST1)
Triassic-Early Jurassic granite and gneiss belt (Thailand) (Tr)
Sibumasu Terrane (2) Carb-Permian Slate Belt (ST2)
Sibumasu Terrane (3) Chaung Mawgyi schists (ST3)
WB EB
Upper Triassic flysch, Jurassic-Cretaceous (?) ophiolites and cherts, over schists, greenstones. WB = Western Belt, EB = Eastern Belt
Tethyan Himalayan Series (THS)
Greater Himalayan Series (GHS)
Lesser Himalayan Series (LHS)
Indo-Burma Ranges
Late Cretaceous-Recent sediments of Central Basin (CB)

1704

Figure 2:

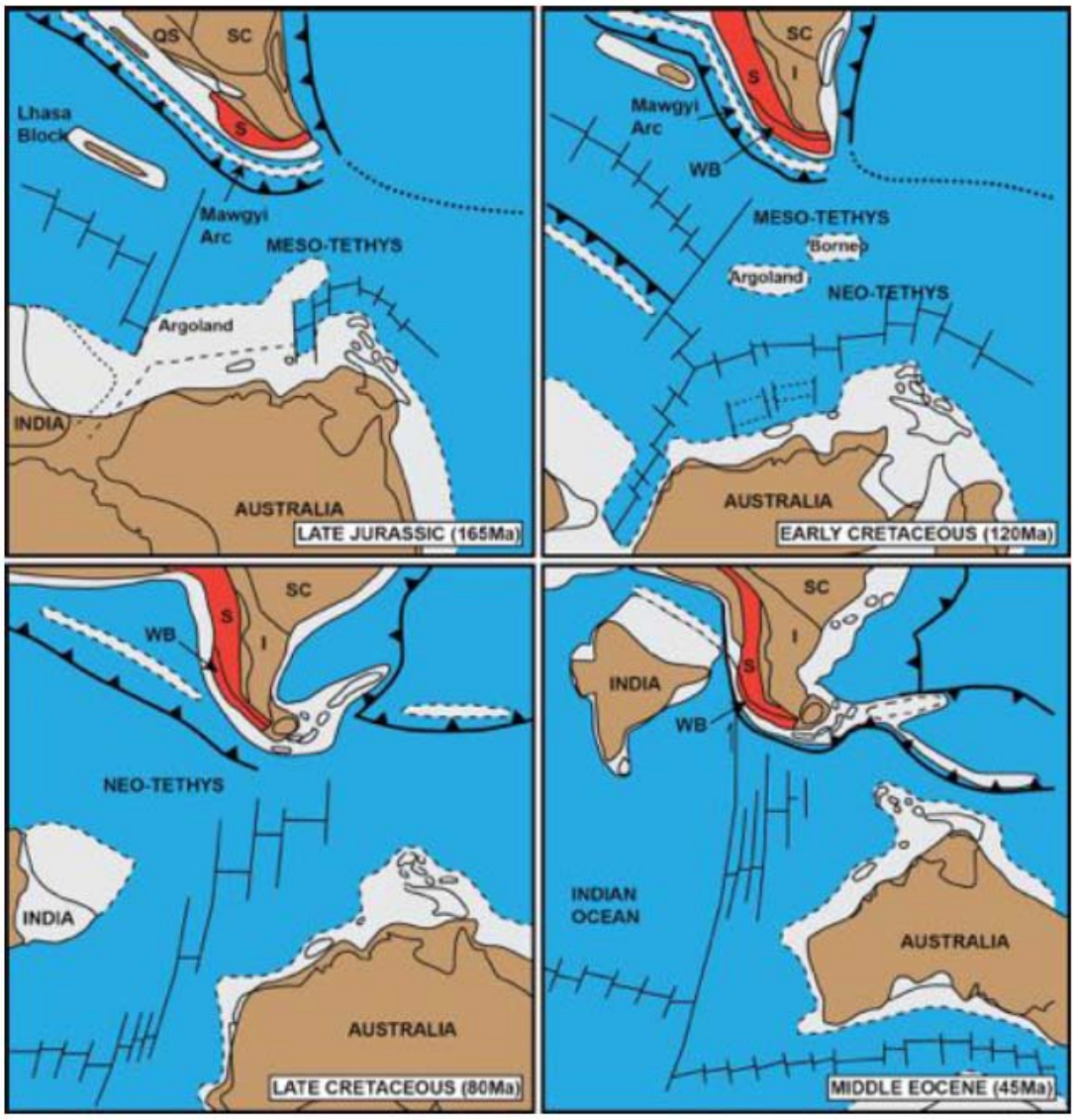

Figure 3:

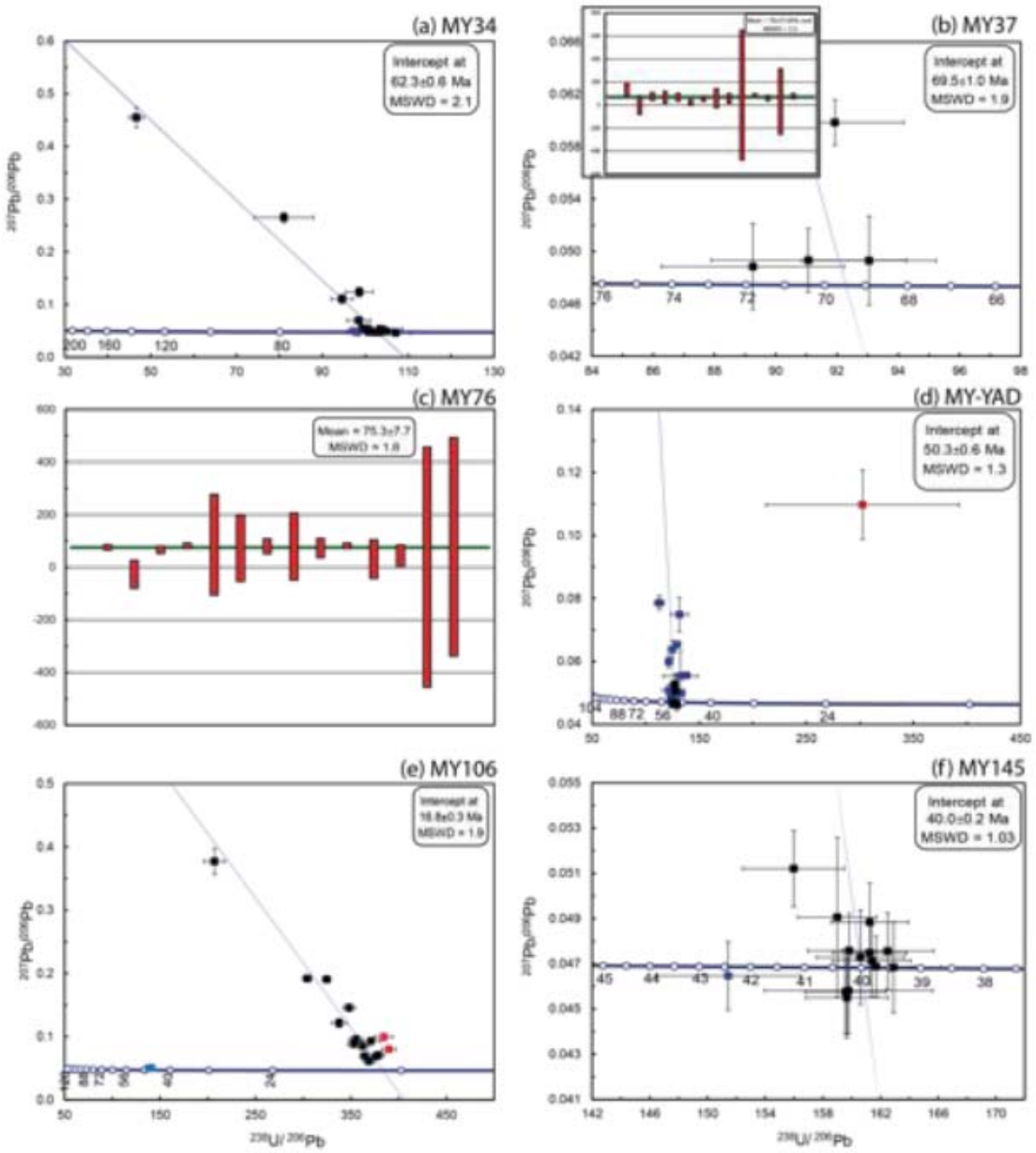
(a) MY34
Intercept at
62.3±0.6 Ma
MSWD = 2.1
(b) MY37
Intercept at
69.5±1.0 Ma
MSWD = 1.9
(c) MY76
Mean = 75.3±7.7
MSWD = 1.8
(d) MY-YAD
Intercept at
50.3±0.6 Ma
MSWD = 1.3
(e) MY106
Intercept at
16.8±0.3 Ma
MSWD = 1.9
(f) MY145
Intercept at
40.0±0.2 Ma
MSWD = 1.03
$^{207}Pb/^{206}Pb$
$^{238}U/^{206}Pb$

Figure 4:

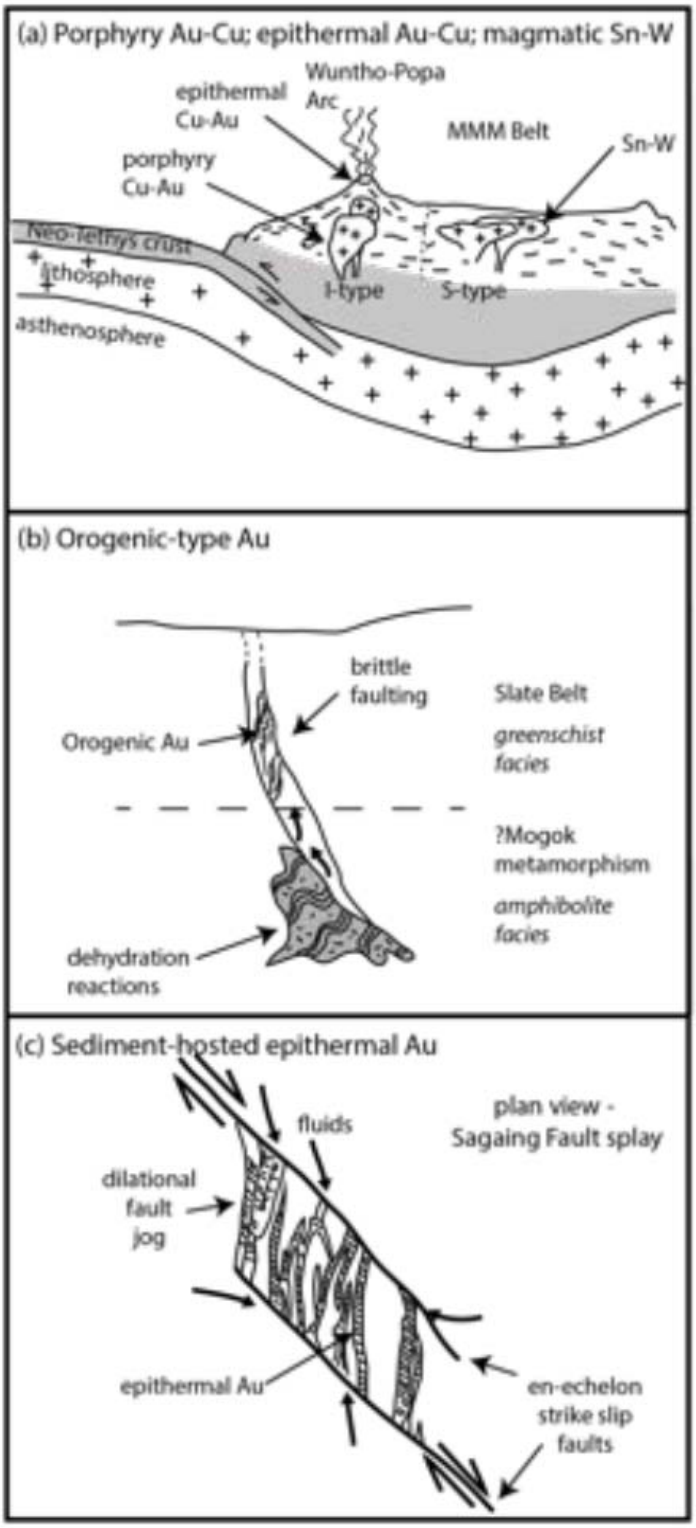
(a) Porphyry Au-Cu; epithermal Au-Cu; magmatic Sn-W
epithermal Cu-Au
Wuntho-Popa Arc
MMM Belt
Sn-W
porphyry Cu-Au
Neo-Tethys crust
lithosphere
asthenosphere
I-type
S-type
(b) Orogenic-type Au
brittle faulting
Slate Belt
greenschist facies
Orogenic Au
?Mogok metamorphism
amphibolite facies
dehydration reactions
(c) Sediment-hosted epithermal Au
plan view - Sagaing Fault splay
fluids
dilational fault jog
epithermal Au
en-echelon strike slip faults

Figure 5:

(a) Accretionary (100-50 Ma)

(b) Collisional (50-30 Ma)

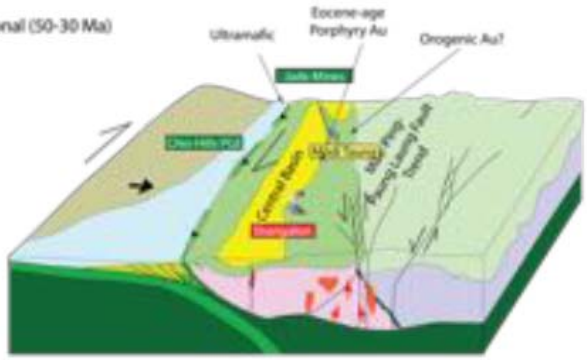

(c) Late Collisional (30-20 Ma)

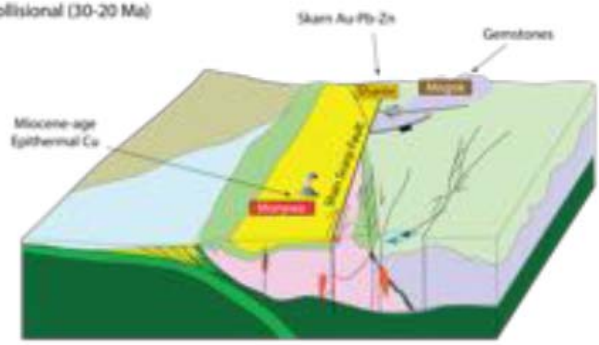

(d) Highly-Oblique Collisional (15-0 Ma)

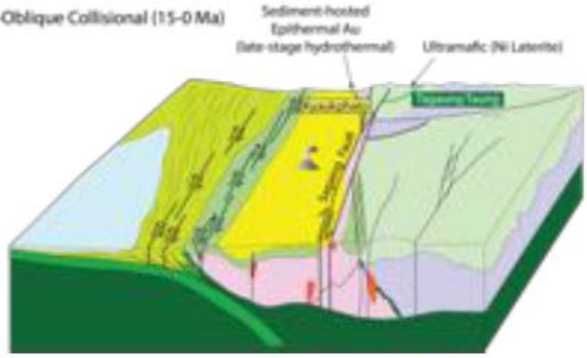

Figure 6:

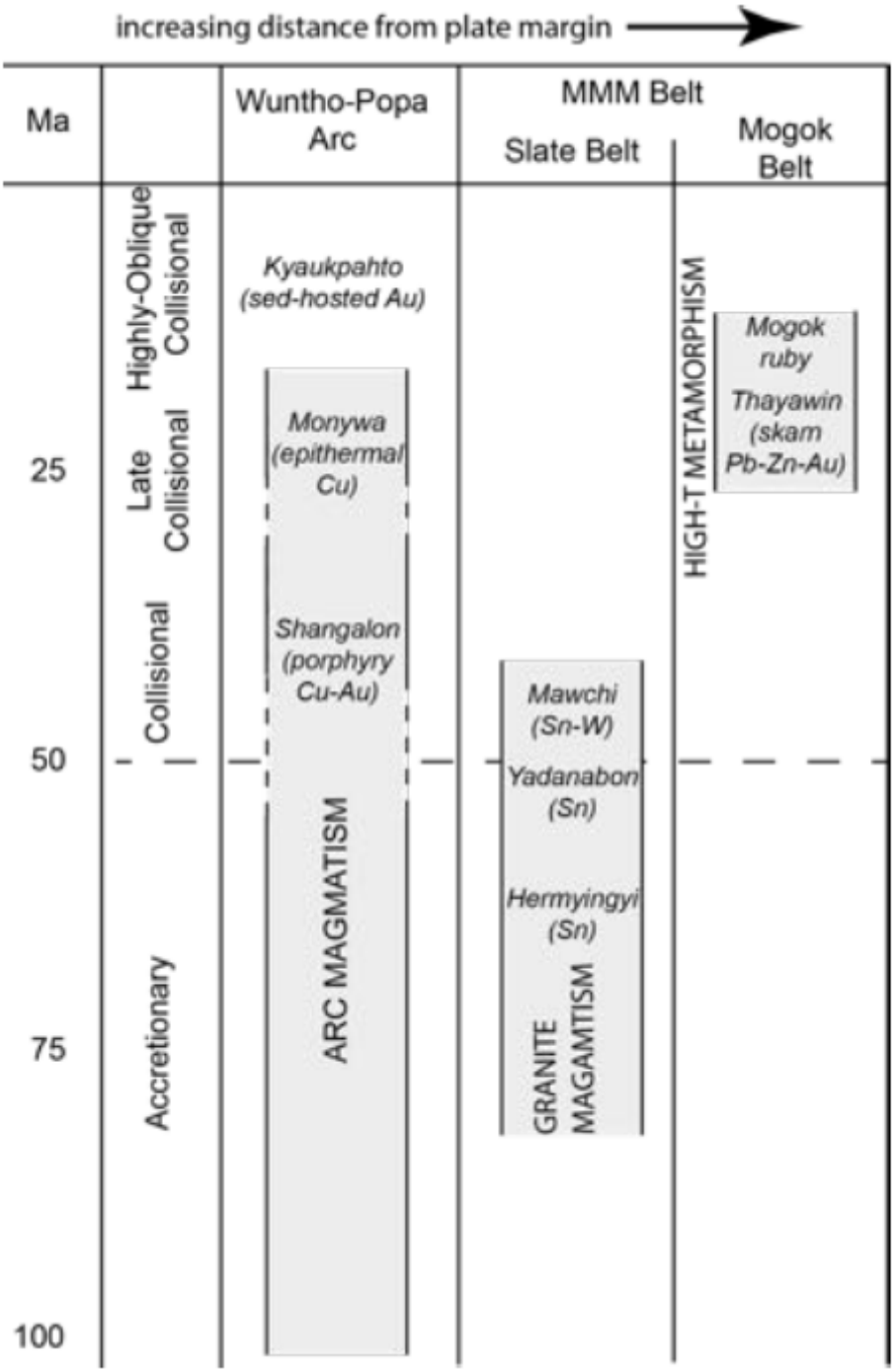
increasing distance from plate margin
Ma
Wuntho-Popa Arc
MMM Belt
Slate Belt
Mogok Belt
Highly-Oblique Collisional
Late Collisional
Collisional
Accretionary
25
50
75
100
Kyaukpahto (sed-hosted Au)
Monywa (epithermal Cu)
Shangalon (porphyry Cu-Au)
ARC MAGMATISM
Mawchi (Sn-W)
Yadanabon (Sn)
Hermyingyi (Sn)
GRANITE MAGAMTISM
HIGH-T METAMORPHISM
Mogok ruby
Thayawin (skarn Pb-Zn-Au)